SURF-ZONE HYDRODYNAMICS

BY

IB A. SVENDSEN
AND
UDAY PUTREVU

RESEARCH REPORT NO. CACR-95-02
FEBRUARY, 1995

CENTER FOR APPLIED COASTAL RESEARCH
OCEAN ENGINEERING LABORATORY
UNIVERSITY OF DELAWARE
NEWARK, DE 19716

Surf-Zone Hydrodynamics

Ib A. Svendsen* Uday Putrevu†

January 24, 1995

1 Introduction

Surf zone dynamics is a highly complicated topic in hydrodynamics which deals with the waves and wave generated phenomena in the region between the breaker line on a beach and the shoreline.

When waves break on a gently sloping beach, large amounts of energy are released and turned into turbulence. As the waves continue breaking and interacting with the bottom topography, the momentum flux of the waves decreases along with the decrease in wave height. The forcing this represents causes the generation of both longer-period waves and currents.

The proper analysis of the dynamics of the surf zone requires a detailed knowledge of the breaking waves and the turbulence they create. This knowledge is not yet available. However, significant progress has been made over the last two decades, in particular, in the area of understanding wave-generated phenomena such as wave set-up, cross-shore and longshore currents and their stability, turbulence and mixing, and the generation of long-wave phenomena (surf beats, edge waves), also termed infragravity waves.

The significant progress made in recent decades is due to the intensive efforts of both experimental and theoretical research. The theoretical modelling was essentially initiated by the discovery of the wave radiation stress in the 60's (Longuet-Higgins & Stewart, 1962, 1964) and has been ongoing with increasing intensity since. The collection of experimental data was mostly limited to laboratory experiments until around 1980 when the first of a series of large field experiments, the Nearshore Sediment Transport Study (NSTS) experiment on two California beaches, was carried out. Since then many such collaborative field experiments, each involving an increasing number of researchers have been conducted, first in the U.S., and later, on a smaller scale, also in Europe and in Japan.

For some time it has been a prevalent perception that the only way to truly understand the complicated processes in the surf zone is through analysis of data from real surf zones in the

*Center for Applied Coastal Research, Department of Civil Engineering, University of Delaware, Newark, DE 19716

†NorthWest Research Associates, Inc., 300 120th Avenue N.E., Bldg. 7, Suite 220, Bellevue, WA 98005

field. The models are far too simple and exclude too many of the important elements of the total picture to be able to illustrate what actually happens on a beach.

On the other hand it has been argued that if you cannot predict even the simplest cases such as a laboratory experiment, then how can you hope to be able to understand and dissect the highly complex picture encountered on a real beach where not only can the important parameters not be controlled but even the most extensive field measuring program will give only a sporadic glimpse of the total picture because it is practically impossible ever to measure enough.

While looking back at the development, however, it is interesting and encouraging to observe that in fact theoretical, laboratory, and field work have all contributed to the new discoveries made over the last decades. The longshore currents and the surf zone set-up were recognized early on in field data but could not be explained properly until the theoretical concept of radiation stress was firmly established. The first quantitative description of the cross-shore circulation and undertow was based on laboratory observations on a barred beach. Both surf beats and shear waves were observed in the field before they were explained theoretically. On the other hand, edge waves were known theoretically long before being observed in the field, and the 3D-vertical structure of currents and infragravity waves are theoretical predictions that, to some extent, still await full verification, as does the nonlinear mechanism of current-current and wave-current interaction. It is characteristic, however, for these and many other phenomena that a strong cross-fertilization between field and modelling efforts has taken place and no uniform pattern for progress or discovery can be identified. The two areas, supplemented by laboratory measurements, form an integral part in the history of progress towards greater understanding of the complicated nature of the area of surf zone dynamics.

It is our impression that, as the modelling efforts have matured to become more complete and complex and the field measurements have revealed increasingly detailed and accurate pictures of the waves and currents, the dichotomy between these two approaches has been nearly wiped out. Hence, it is likely that, in the not too distant future, models will be able to provide additional and accurate information about details that were actually not measured in a given field experiment and also assist in the planning of new field experiments.

Today so many contributions have been made towards our understanding of the surf zone that it will be impossible, in one review paper, to cover them all. Therefore, the presentation here will, in spite of all efforts to the contrary, have to leave out, or only cover sporadically, important parts of the picture. In selecting the material for this paper, we have undoubtedly been biased by our own firm association with the theoretical or modelling side of the topic but even there many papers have not been included.

In this review we have chosen to concentrate on "recent progress." Thus, we have chosen not to include material that is readily available in standard text books (Phillips 1977, Mei 1983). A consequence of this choice is that the paper makes only passing references to some of the pioneering works (*e.g.*, Longuet-Higgins & Stewart 1962, 1964; Bowen *et al.* 1968; Bowen 1969a; Thornton 1970; Longuet-Higgins 1970; and many others).

In addition to the books by Phillips and Mei, the reader is referred to review papers by Peregrine (1983), Battjes (1988), and Battjes *et al.* (1990) for recent overviews (sometimes from a different perspective) of some of the material covered here. Basic material about boundary layers in non-breaking waves may be found in Nielsen (1992), but very little is available about boundary layers under breaking waves. Some information about wave boundary layers may also be found in texts more specifically oriented towards sediment transport such as Sleath (1984) and Fredsoe & Deigaard (1993).

The paper is organized as follows. The rest of this section is devoted to describing the basic assumptions involved in the analysis of surf zone motions. In Section 2, we outline the derivation of the "short-wave-averaged" equations in the nearshore. The equations given in that section are valid for vertically nonuniform current motions and are hence generalized forms of the equations given by Phillips and Mei. Section 3 discusses our present state of knowledge of the short-wave motion in the surf zone. A brief discussion of bottom boundary layers and bottom shear stresses is given in Section 4. The present state of understanding of steady circulation patterns (including the decay of short-waves, longshore currents, and undertow) are reviewed in Section 5. Sections 6 and 7 are devoted to discussing infragravity and shear waves, respectively. Section 8 discusses Quasi 3D comprehensive models, and the paper concludes with a summary in Section 9.

Basic Assumptions

The direct approach to describing and analyzing surf zone phenomena would require solution of the hydrodynamical equations for the conservation of mass and momentum. Since the flow is highly turbulent due to the wave breaking and since the free surface introduces essential non-linearities, this task has not been accomplished yet.

Whereas there have been many attempts towards this goal, two major approaches have been pursued with particular success. One particularly aims at describing the pattern of currents and long ('infragravity') wave motion generated by the ('short') storm waves or swell. This approach is based on versions of the hydrodynamical equations which are averaged over the short wave period so that in these equations only the mean effect (over a wave period) of the short waves such as net mass, momentum and energy fluxes, are included in the equations.

The second approach solves the hydrodynamical equations in the time domain but only in the horizontal plane. This is made possible by approximate representations in the equations of the variations of pressure and velocity fields in the vertical direction based on the assumption that the horizontal length scale of the wave motion is much larger than the water depth. It leads to the class of descriptions that include the nonlinear shallow-water equations, Boussinesq models, and derivatives thereof.

A fundamental assumption which underlies all these efforts is the concept of a gently sloping bottom which is normally the case on littoral beaches. The gentleness of the bottom slope is used to assume that, at each location of the region, the local short-wave motion is in equilibrium with the local values of the the depth, the wave height, and wave period.

It turns out that this concept of gentleness is related both to the bottom slope h_x and to the wavelength L. Analysis of the effect the bottom has on the wave motion shows that to the first order this effect is proportional to the dimensionless beach slope parameter

$$S = \frac{h_x\, L}{h} \tag{1}$$

Here L is a 'local' wave length evaluated as $L = cT$ where c is the local phase velocity of the wave, T its period. Since $h_x\, L = \Delta h$ is the (first Taylor approximation to the) change in depth over one wave length, we see that S is the *relative* change in depth over that distance.

Hence, we may conclude that if we want to be able to *neglect* the effect that a sloping bottom has on the local wave motion (i.e., to assume "locally constant depth"), we should assume conditions that everywhere satisfy the requirement that

$$S \ll 1 \tag{2}$$

This will also ensure that the assumption of no reflection of wave energy by the bottom topography is reasonable. In practice, this usually is assumed to be satisfied if $S \leq 1$ though for some results $S < 0.3$–0.5 is probably necessary. For the larger S-values, we can expect that the wave behavior will depend on the value of S. This problem, however, has not really been discussed in the literature yet.

2 The Short-Wave-Averaged Equations

2.1 Introduction

In this section we give a brief account of the depth-integrated, time-averaged equations for conservation of mass and momentum. The equations are presented here for currents that are non-uniform over the depth. This is a more general form than that given for example by Phillips (1977) or Mei (1983).

Similar equations can be derived for the conservation of total energy, the conservation of oscillatory (wave) energy and the conservation of mean (current) energy; however, non-uniform versions of the energy equations have not been presented in the literature at the present time. For the general form of the depth uniform versions of these equations the reader is referred to the book by Phillips (1977).

In this section we also discuss the local wave-averaged equations used to determine the vertical variation of the current and long wave particle velocities in short-wave-averaged models.

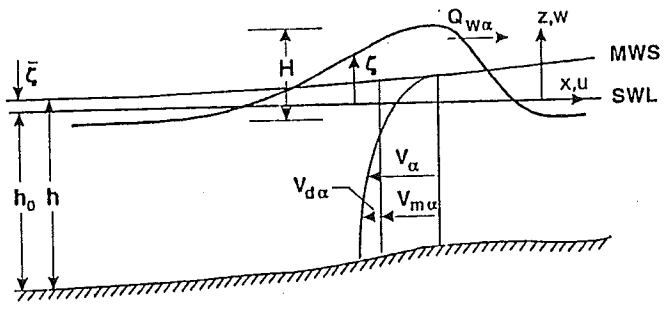

Figure 1: Sketch defining the various geometrical quantities used in this paper.

2.2 Description of the Derivation

The depth-integrated, time-averaged equations are derived from the Reynolds equations for conservation of mass

$$\frac{\partial u_\alpha}{\partial x_\alpha} + \frac{\partial w}{\partial z} = 0 \tag{3}$$

and momentum

$$\frac{\partial u_\beta}{\partial t} + \frac{\partial u_\alpha u_\beta}{\partial x_\alpha} + \frac{\partial u_\beta w}{\partial z} = -\frac{1}{\rho}\frac{\partial p}{\partial x_\beta} + \frac{1}{\rho}\left(\frac{\partial \tau_{\alpha\beta}}{\partial x_\alpha} + \frac{\partial \tau_{z\beta}}{\partial z}\right) \tag{4}$$

$$\frac{\partial w}{\partial t} + \frac{\partial u_\alpha w}{\partial x_\alpha} + \frac{\partial w^2}{\partial z} = -\frac{1}{\rho}\frac{\partial p}{\partial z} + \frac{1}{\rho}\left(\frac{\partial \tau_{\beta z}}{\partial x_\beta} + \frac{\partial \tau_{zz}}{\partial z}\right) \tag{5}$$

Here x_α, z are horizontal and vertical coordinates, respectively; u_β represents the total particle velocity in the horizontal direction; w, the vertical component of the total velocity; p, the pressure; and $\tau_{\alpha\beta}$, the turbulent shear stresses. Figure 1 shows the definition of the geometrical quantities used throughout this paper.

The derivation of the short-wave-averaged equations requires the following series of operations:

- The continuity equation and the horizontal components of the momentum equations are integrated from the bottom $-h_0$ to the instantaneous free surface ζ.
- This yields terms of the form $\int \frac{\partial}{\partial t}, \int \frac{\partial}{\partial x_\alpha}$, etc., in the equations. Leibnitz's rule is used to transform those terms into terms of the form $\frac{\partial}{\partial t}\int, \frac{\partial}{\partial x_\alpha}\int$, etc.

- These steps leave a number of other terms in the equations evaluated at $-h_0$ and ζ. Invoking the exact boundary conditions at the bottom and the free surface essentially eliminate all these terms except for the normal and tangential stresses at the boundaries.
- Integrating the vertical momentum equation from the free surface to a level z gives an expression for the pressure p at level z. This can be used to eliminate the pressure from the horizontal momentum equations.
- Finally, the equations are averaged over the short-wave period. In describing the result of this process we use $\overline{}$ to indicate time averaging, which means that

$$\bar{\cdot} = \frac{1}{T}\int_t^{t+T} \cdot \, dt \tag{6}$$

where T is the wave period.

2.3 The Equations

Before eliminating the pressure, the depth-integrated equations of continuity and momentum can be written as

Continuity

$$\frac{\partial \bar{\zeta}}{\partial t} + \frac{\partial \bar{Q}_\alpha}{\partial x_\alpha} = 0 \tag{7}$$

where $\bar{Q}_\alpha$ is the total volume flux through a vertical section defined by

$$\bar{Q}_\alpha = \overline{\int_{-h_o}^{\zeta} u_\alpha \, dz} \tag{8}$$

Momentum

$$\rho\overline{\frac{\partial}{\partial t}\int_{-h_0}^{\zeta} u_\beta dt} + \rho\frac{\partial}{\partial x_\alpha}\overline{\int_{-h_0}^{\zeta}\left(u_\alpha u_\beta - \tau_{\alpha\beta}\right) dz} + \frac{\partial}{\partial x_\beta}\left(\overline{\int_{-h_0}^{\zeta} p dz} - \frac{1}{2}\rho g h^2\right)$$
$$= \rho g\left(\bar{\zeta} + h_0\right)\frac{\partial \bar{\zeta}}{\partial x_\beta} + \overline{\tau_\beta^S} - \overline{\tau_\beta^B} \tag{9}$$

The velocity u_α represents the total instantaneous (horizontal) fluid velocity at a point, and the vertical distribution of this velocity has not yet been specified. $\overline{\tau_\beta^s}$ and $\overline{\tau_\beta^B}$ are the time-averaged surface and bottom shear stresses, respectively. As before, $\tau_{\alpha\beta}$ are the turbulent shear stresses (Reynolds stresses).

To bring the momentum equation into a more useful form, we separate the total velocity (u_α, w) into a "current" and a short-wave component by letting

$$u_\alpha(=\widehat{u_\alpha}) = V_\alpha + u_{w\alpha} \;\; ; \;\; w(=\widehat{w}) = w_w \tag{10}$$

Here $u_{w\alpha}$, w_w are the short-wave components which have

$$\overline{u_{w\alpha}} \, , \, \overline{w_w} = 0 \qquad \text{below wave-trough level} \tag{11}$$

and V_α is the current. $\overline{\cdot}$ represents turbulent averaging of the quantity. If the short waves are irregular, we will expect the "current" to be varying with time. $V_\alpha(t)$ may then be equivalent to a long wave particle velocity.

We also introduce the radiation stress $S'_{\alpha\beta}$ defined by

$$S'_{\alpha\beta} \equiv \overline{\int_{-h_0}^{\zeta} (\rho u_{w\alpha} u_{w\beta} + p\delta_{\alpha\beta})\, dz} - \delta_{\alpha\beta}\frac{1}{2}\rho g h^2 \tag{12}$$

The momentum equation can then be written[1]

$$\begin{aligned} &\rho\frac{\partial}{\partial t}\bar{Q}_\beta + \rho\frac{\partial}{\partial x_\alpha}\int_{-h_0}^{\bar{\zeta}} V_\alpha V_\beta dz + \rho\frac{\partial}{\partial x_\alpha}\overline{\int_{\zeta_t}^{\zeta} u_{w\alpha}V_\beta + u_{w\beta}V_\alpha dz} \\ &\quad +\rho g(\bar{\zeta}+h_0)\frac{\partial\bar{\zeta}}{\partial x_\beta} + \frac{\partial}{\partial x_\alpha}\left[S'_{\alpha\beta} - \overline{\int_{-h_0}^{\zeta}\tau_{\alpha\beta}dz}\right] \\ &\quad -\tau^S_\beta + \tau^B_\beta = 0 \end{aligned} \tag{13}$$

In this form of the equation, we have grouped the $S'_{\alpha\beta}$ term, which is the wave contribution, and the $\tau_{\alpha\beta}$ term, which is the turbulent contribution to the momentum flux. This grouping emphasizes the parallel mechanism behind these two terms, one caused by organized (wave) fluctuations, the other by disorganized (turbulent) fluctuations. In fact, in some texts this is further emphasized by using the same letter "S" for the two contributions

Wave radiation stress	$S'_{\alpha\beta}$
Turbulent "radiation stress"	$S'^t_{\alpha\beta} = -\overline{\int_{-h_0}^{\zeta}\tau_{\alpha\beta}dz}$

It is important at this point to emphasize that the only approximations that have been made in the derivation of these equations, apart from the usual approximations associated with fluid flow, are associated with neglecting vertical components of bottom and surface stresses (gently sloping boundaries).

Depth Uniform Currents

Equation (13) allows the currents to vary over depth, and in fact we know today not only that nearshore currents normally do so but that this depth variation is an important part of the mechanism that controls the horizontal distribution of nearshore circulation.

[1]The derivation of this equation for the depth-uniform currents is given by Mei (1983). However, he finds it necessary to require ∇h_0 small to obtain the result because of an inappropriate use of the result for the pressure at an arbitray (x-independent) level z to determine the pressure at the (x-dependent) bottom level $-h_0$.

However, making the assumption of depth-uniform currents allows us to simplify (22) somewhat. Introducing the assumption that V_α, V_β are independent of z (22) takes the form

$$\rho\frac{\partial \bar{Q}_\beta}{\partial t}+\frac{\partial}{\partial x_\alpha}\left(\rho\frac{\bar{Q}_\alpha\bar{Q}_\beta}{h}+S_{\alpha\beta}-\overline{\int_{-h_0}^{\zeta}\tau_{\alpha\beta}dz}\right)=-\rho g h\frac{\partial\bar{\zeta}}{\partial x_\beta}+\tau_\beta^S-\tau_\beta^B \tag{14}$$

valid for depth-uniform currents only. In this form of the horizontal momentum equation, the radiation stress $S_{\alpha\beta}$ is given by (23)

The form (14) is equivalent to the momentum equation used by Phillips with addition of the turbulent stresses $\tau_{\alpha\beta}$, and the horizontal components of the surface stress τ_β^S and the bottom shear stress τ_β^B, all of which are neglected by Phillips.

Different Forms of the Momentum Equation for Depth-Varying Currents

The momentum equation (13) is written in terms of V_α, which is the current defined in the traditional way: the net velocity at any point below wave-trough level over and above the purely oscillatory wave motion. For the general case of depth-varying currents, it is convenient to split this current into a depth-uniform and depth-varying part, and it turns out that it is relevant to consider two different ways of doing this.

One way of splitting the current is by defining a V_1 such that

$$V_\alpha=\frac{\bar{Q}_\alpha}{h}+V_{1\alpha}(z) \tag{15}$$

Closer inspection shows that

$$\int_{-h_0}^{\bar{\zeta}}V_{1\alpha}dz=-Q_{w\alpha} \tag{16}$$

If we introduce this definition into (13), the momentum equation can be written as

$$\begin{aligned}&\rho\frac{\partial}{\partial t}\bar{Q}_\beta+\rho\frac{\partial}{\partial x_\alpha}(\frac{\bar{Q}_\alpha\bar{Q}_\beta}{h})+\rho\frac{\partial}{\partial x_\alpha}\int_{-h_0}^{\bar{\zeta}}V_{1\alpha}V_{1\beta}dz\\&+\rho\frac{\partial}{\partial x_\alpha}\overline{\int_{\zeta_t}^{\zeta}u_{w\alpha}V_{1\beta}+u_{w\beta}V_{1\alpha}dz}+\rho g(\bar{\zeta}+h_0)\frac{\partial\bar{\zeta}}{\partial x_\beta}\\&+\frac{\partial}{\partial x_\alpha}\left[S'_{\alpha\beta}-\overline{\int_{-h_0}^{\zeta}\tau_{\alpha\beta}dz}\right]-\tau_\beta^S+\tau_\beta^B=0\end{aligned} \tag{17}$$

Alternatively, the current may be divided by defining $V_{m\alpha}$ by

$$V_{m\alpha}=\frac{\bar{Q}_\alpha-Q_{w\alpha}}{h} \tag{18}$$

where

$$Q_{w\alpha} = \overline{\int_{-h_0}^{\zeta} u_{w\alpha}\, dz} \tag{19}$$

so that the depth-varying part, V_d, of the current can be defined by

$$V_\alpha = V_{m\alpha} + V_{d\alpha}(z) \tag{20}$$

It may be verified that

$$\int_{-h_0}^{\bar{\zeta}} V_{d\alpha} dz = 0 \tag{21}$$

Then (13) may be written as

$$\begin{aligned} &\rho\frac{\partial}{\partial t}\bar{Q}_\beta + \rho\frac{\partial}{\partial x_\alpha}(\frac{\bar{Q}_\alpha\bar{Q}_\beta}{h}) + \rho\frac{\partial}{\partial x_\alpha}\int_{-h_0}^{\bar{\zeta}} V_{d\alpha}V_{d\beta}dz \\ &+\rho\frac{\partial}{\partial x_\alpha}\overline{\int_{\zeta_t}^{\zeta} u_{w\alpha}V_{d\beta} + u_{w\beta}V_{d\alpha}dz} + \rho g(\bar{\zeta}+h_0)\frac{\partial\bar{\zeta}}{\partial x_\beta} \\ &+\frac{\partial}{\partial x_\alpha}\left[S_{\alpha\beta} - \overline{\int_{-h_0}^{\zeta}\tau_{\alpha\beta}dz}\right] - \tau_\beta^S + \tau_\beta^B = 0 \end{aligned} \tag{22}$$

where $S_{\alpha\beta}$ is a radiation stress defined by

$$S_{\alpha\beta} = S'_{\alpha\beta} - \rho\frac{Q_{w\alpha}Q_{w\beta}}{h} \tag{23}$$

Discussion

Before we discuss the differences between the forms of equations (17) and (22), it is worthwhile to discuss the role of various terms in these equations. In both these equations, the first term represents the temporal acceleration and the second term represents the convective accelerations. The $\partial\bar{\zeta}/\partial x_\beta$ term represents the pressure gradients; $S_{\alpha\beta}$ and $\tau_{\alpha\beta}$ terms represent the interaction between the mean flow and the short waves and turbulence, respectively. τ_β^S represents the applied surface shear stress and τ_β^B the bottom stress. Finally, the two integral terms represent current-current and wave-current interaction terms.

We see that the two definitions of how the current is divided into a depth-uniform and a depth-varying part are closely connected to two different definitions of the radiation stress, the first of which is the definition given by (12), the second is given by the expression (23). In both cases the nonlinear interaction terms have been separated into a contribution which is equivalent to the only nonlinear term for depth uniform currents in (14) and a set of integrals that only contain contributions from the waves and the depth varying part of the currents.

We notice that the two forms are equivalent in the sense that the structural forms are exactly the same. The differences only occur in the definitions of the radiation stress and the way in which

the current has been divided into a depth-uniform and a depth-varying part. The form (22) and the variables used in that equation correspond to a generalized version of the form introduced by Phillips (1977). Similarly, (17) resembles the momentum equation given by Mei (1983) generalized to non-uniform currents. The algebraic similarity between (12) and Mei's radiation stress is somewhat formal, however, because Mei uses a different definition of $u_{w\alpha}$ and also neglects the $Q_{w\alpha}Q_{w\beta}/h$ -term. Mei defines the wave particle velocity by requiring $\overline{\int_{-h_0}^{\zeta} u_{w,Mei}dz} = 0$. This implies that the return current is included in his definition of the wave particle velocity. Hence, in our notation, $u_{w,Mei} = u_w - Q_w/h$. Quite paradoxically, it turns out that substituting this into Mei's expression for the radiation stress we obtain an expression identical to (23). Or, in other words, the effect of using a different wave particle velocity in the definition of the radition stress (as Mei does) is balanced by the omission of the $Q_{w\alpha}Q_{w\beta}/h$ -term.

Comparing with (23), we see that the difference between the equations (17) and (22) and the equivalent equations for depth-uniform currents is represented by the current-current and wave-current interaction terms

$$\rho\frac{\partial}{\partial x_\alpha}\int_{-h_0}^{\bar{\zeta}} V_{1\alpha}V_{1\beta}dz + \rho\frac{\partial}{\partial x_\alpha}\overline{\int_{\zeta_t}^{\zeta} u_{w\alpha}V_{1\beta} + u_{w\beta}V_{1\alpha}dz} \quad in(17) \tag{24}$$

and

$$\rho\frac{\partial}{\partial x_\alpha}\int_{-h_0}^{\bar{\zeta}} V_{d\alpha}V_{d\beta}dz + \rho\frac{\partial}{\partial x_\alpha}\overline{\int_{\zeta_t}^{\zeta} u_{w\alpha}V_{d\beta} + u_{w\beta}V_{d\alpha}dz} \quad in(22) \tag{25}$$

These terms essentially represent the contribution from the depth variation of the current velocities. Little is known about the importance of these terms except that it is from these terms the dispersive mixing originates; this dispersive mixing appears to give important contributions to the lateral mixing for longshore currents (see section 5.2 for further discussion).

Another issue which needs some discussion is the choice of ζ_t, the wave-trough level, as lower limit for the integrations around the surface. This clearly is a logical choice because above that level there is only water part of the time so that it becomes questionable how the mean velocity (the current) should be defined in that region. It is also clear, however, from (13) that this choice does not free us from identifying what is wave and what is current above ζ_t, since it has not been possible to write the integral above that level in terms of the total velocities only and at the same time extract the wave part (which is part of the radiation stress).

Hence it is necessary to separate the flow above trough level into wave and current part no matter which choice of integration limit we make. If we use $\bar{\zeta}$ as the limit for the second integral in (13), it is necessary to remember that to get an equation similar to (13) with $\bar{\zeta}$ as the lower integration limit in the second integral it will be necessary to assume that the $u_{w\alpha}$ we then define between ζ_t and $\bar{\zeta}$ satisfies (11), which means assuming $u_{w\alpha}$ defined also when there is no water above the trough. In order to generate the correct integral, the current V_α given by (10) would then have to be defined as the difference between the total (actual physical) velocity and the wave component. This implies that during the period where there is no water the current would be minus the assumed wave component.

In contrast to this, using ζ_t as the lower limit of the second integral in (13) allows us to define both the wave and the current component of the total velocity only during the period of time when there actually is water. This is our reason for choosing ζ_t as the integration limit. As mentioned earlier, however, we still have to make the separation between wave and current part whether we choose ζ_t or ζ as integration limit. We also emphasize that (17) and (22) are still exact in the same sense as (13).

2.4 The Energy Equation

The energy equation for the combined wave and current motion is needed in wave-averaged models to determine the wave height variation and it can be derived by the same depth integration and time-averaging processes outlined for the momentum equation. In its general form, the energy equation is even more complicated than the momentum equation (13).

For a derivation for the case of depth-uniform currents, reference is made to Phillips (1977). In this general form, the energy equation includes a number of terms describing the interaction between the short-wave motion and the currents/long wave motion. These current terms, however, are usually of minor importance for the simple applications discussed here. If restricted to the wave motion only, the energy equation simply reads

$$\frac{\partial E_{f,\alpha}}{\partial x_\alpha} = \mathcal{D} \tag{26}$$

Here, $E_{f\alpha}$ is the energy flux of the short waves in the x_α direction and $\mathcal{D}$ is the energy dissipation per unit time and area of bottom.

The energy flux for the waves is an abbreviation for a number of terms that emerge through the derivation of the equation. It is defined as

$$E_{f\alpha} = \overline{\int_{-h_o}^{\zeta} \left(\rho\, g z + p + \frac{1}{2}\rho(u_w^2 + v_w^2 + w_w^2) \right) u_{w\alpha} dz} \tag{27}$$

For sine waves, (27) yields the well known result

$$E_f = \frac{1}{16}\, \rho\, g\, c\, H^2 (1 + G) \tag{28}$$

where $G = \frac{2kh}{sinh2kh}$ The dissipation of energy $\mathcal{D}$ can be described by the work done by internal (turbulent) stresses, but this does not lead to a viable means of determining $\mathcal{D}$ from our present knowledge of the wave motion.

Note that in (26) energy dissipation corresponds to $\mathcal{D} < 0$. The practical evaluation of $E_{f,\alpha}$ and $\mathcal{D}$ is discussed in more detail in Sections 3.

2.5 Wave-Averaged Quantities

As we have seen in equations (7), (22) and (26) describing the wave generated currents and long-wave phenomena, the effects of the short waves are represented by the volume flux, Q_w, due to the wave motion; the excess momentum flux or radiation stress, $S_{\alpha\beta}$; and the energy flux, $E_{f,\alpha}$. An essential aspect of the definitions of these quantities is that they are exact in the sense that if we substitute exact short-wave expressions for the velocities and pressures in these definitions then we get the exact results for Q_w, $S_{\alpha\beta}$, and $E_{f,\alpha}$. The difficulty of course is that we do not have such exact results for the short-wave motion, in particular in the surf zone. Therefore, it is important to realize that the approximation used instead for the short-wave motion is one of the major sources of inaccuracy in the prediction of nearshore circulation. An additional, important wave-averaged quantity is the energy dissipation $\mathcal{D}$ caused by the wave breaking.

To be able to predict steady nearshore circulation and long-wave phenomena from the averaged models in the surf zone, these quantities must be expressed in terms of wave height, wave period, water depth, etc.

The Radiation Stress

The radiation stress is by far the most complicated of these quantities. For reference, it is worth noticing that it can be written in several useful forms. Thus, if we eliminate the pressure from (12) using the vertically integrated vertical component of the momentum equation, we get

$$S_{\alpha\beta} = \rho \overline{\int_{-h_0}^{\zeta} \left[u_{w\alpha} u_{w\beta} - \delta_{\alpha\beta} \left(w_w^2 + \widetilde{w'^2} \right) \right] dz} + \frac{1}{2} \rho g \overline{\eta^2} - \rho \frac{Q_{w\alpha} Q_{w\beta}}{h} \tag{29}$$

where w' is the vertical component of the turbulent velocity fluctuations.

In the vertical plane of the direction of wave propagation the wave-induced particle velocities are

$$u = (u_w^2 + v_w^2)^{1/2} \tag{30}$$

$$w = w_w \tag{31}$$

and the mass flux is

$$Q_w = (Q_{wx}^2 + Q_{wy}^2)^{1/2} \tag{32}$$

We can then define (the scalars)

$$S_m = \overline{\int_{-h_o}^{\zeta} \rho u^2 \, dz} - \rho \frac{Q_w^2}{h} \tag{33}$$

$$S_p = -\overline{\int_{-h_o}^{\zeta} \rho \, w^2 + \widetilde{w'^2} dz} + \frac{1}{2} \rho g \overline{\eta^2} \tag{34}$$

so that

$$S_r = S_m + S_p \tag{35}$$

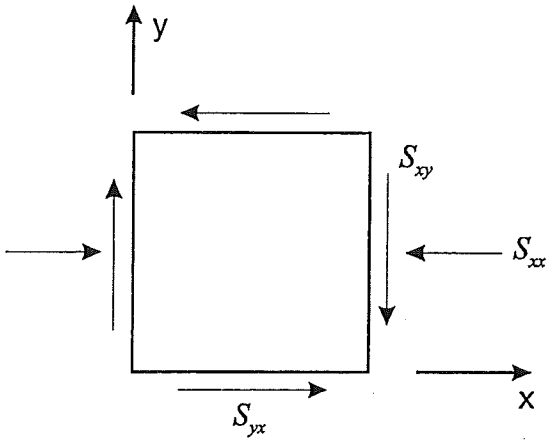

Figure 2: Positive directions for the radiation stress components. Note that the positive directions for the radiation stresses are opposite to the normal positive directions for stresses.

represents the radiation stress on a vertical surface with the normal vector in the direction of wave propagation.

The four components of $S_{\alpha\beta}$ that represents the radiation stress elements parallel and perpendicular to the x, y axes can then be written

$$S_{\alpha\beta} = S_m \, e_{\alpha\beta} + S_p \delta_{\alpha\beta} \tag{36}$$

where

$$e_{\alpha\beta} = \left\{ \begin{array}{ll} \cos^2 \alpha_w & \sin \alpha_w \cos \alpha_w \\ \sin \alpha_w \cos \alpha_w & \sin^2 \alpha_w \end{array} \right\} \tag{37}$$

Hence, from the results S_m and S_p for the radiation stress components on a surface perpendicular to the direction of wave propagation, it is possible to determine the radiation stress $S_{\alpha\beta}$ in any direction.

Notice that the negative sign in front of the $\tau_{\alpha\beta}$ term in (13) indicates the difference between the positive sign on the $u_\alpha u_\beta$ term in the traditional definition (12) for $S_{\alpha\beta}$ and the negative sign on the $u_\alpha u_\beta$ term in the definition normally adopted for $\tau_{\alpha\beta}$. This implies that the sign convention for $S_{\alpha\beta}$ and $\tau_{\alpha\beta}$ is opposite—a point worth bearing in mind when checking direction of terms in the equations. The positive directions are shown in Fig. 2.

Dimensionless parameters for wave-averaged quantities

Without loss of generality, in the wave direction we may write the wave parameters in the

following way

$$Q_w = c\frac{H^2}{h}B_Q \tag{38}$$

$$S_r = \rho\, g\, H^2 P \tag{39}$$

$$E_f = \rho\, g\, c\, H^2 B \tag{40}$$

$$\mathcal{D} = g\,\frac{H^3}{4hT}D \tag{41}$$

Essentially, these expressions define dimensionless parameters B_Q, P, B and D for the four wave-averaged quanties that appear in the depth-integrated, short-wave-averaged equations. In a simplified manner, one can say that the dimensional components h, H, T and c in (38)–(41) measure the size of the wave motion, whereas the dimensionless parameters are measures of the shape of the wave motion (understood as surface profile, velocity and pressure fields, etc.).

One of the important questions is how accurate are the approximations (such as sine wave theory) normally used for calculating these quantities? This is discussed in section 3.4.

2.6 The Local Wave-Averaged Equations

The local wave-averaged equations are essentially the Reynolds equations (4) in which we split the total velocity u_α into a short-wave and a current component by substituting (10) for u_α followed by a short-wave averaging. The result for the current motion can be written (see Svendsen & Lorenz, 1989)

$$\frac{\partial U_\beta}{\partial t} + \frac{\partial U_\alpha U_\beta}{\partial x_\alpha} + \frac{\partial U_\beta W}{\partial z} + \frac{\partial(\overline{u_{w\alpha}u_{w\beta}} - \overline{w_w^2})}{\partial x_\alpha} + \frac{\partial \overline{u_{w\beta}w_w}}{\partial z} = -g\frac{\partial \overline{\zeta}}{\partial x_\beta} + \frac{1}{\rho}\left(\frac{\partial \tau_{\alpha\beta}}{\partial x_\alpha} + \frac{\partial \tau_{z\beta}}{\partial z}\right) \tag{42}$$

Usually, the turbulent shear stresses $\tau_{\alpha\beta}$ in this equation are modelled by an eddy-viscosity assumption and it is also assumed that W is negligible. The resulting equation reads

$$\frac{\partial U_\beta}{\partial t} + \frac{\partial U_\alpha U_\beta}{\partial x_\alpha} + \frac{\partial(\overline{u_{w\alpha}u_{w\beta}} - \overline{w_w^2})}{\partial x_\alpha} + \frac{\partial \overline{u_{w\beta}w_w}}{\partial z} =$$

$$-g\frac{\partial \overline{\zeta}}{\partial x_\beta} + \frac{1}{\rho}\frac{\partial}{\partial x_\alpha}\left(\nu_t\left(\frac{\partial U_\alpha}{\partial x_\beta} + \frac{\partial U_\beta}{\partial x_\alpha}\right)\right) + \frac{1}{\rho}\frac{\partial}{\partial z}\left(\nu_t\frac{\partial U_\beta}{\partial z}\right) \tag{43}$$

Special forms of this equation have been solved for the vertical distribution of the current velocity U_β. Thus the simplest case of steady, one-dimensional cross-shore circulation on a straight

beach leads to a description of the undertow current, see Section 5. Also discussed in that section are other special cases, such as the vertical distribution of the longshore current on a long straight beach and the nonlinear interaction between cross-shore and longshore currents (leading to the concept of dispersive mixing). Section 5.4 also includes a brief discussion of the boundary conditions used for solving (43). The time-varying velocity profiles in infragravity surf-beats (the special cross-shore form of infragravity waves in general) are discussed in Section 6.5. These results are all derived as solutions to special cases described by (43).

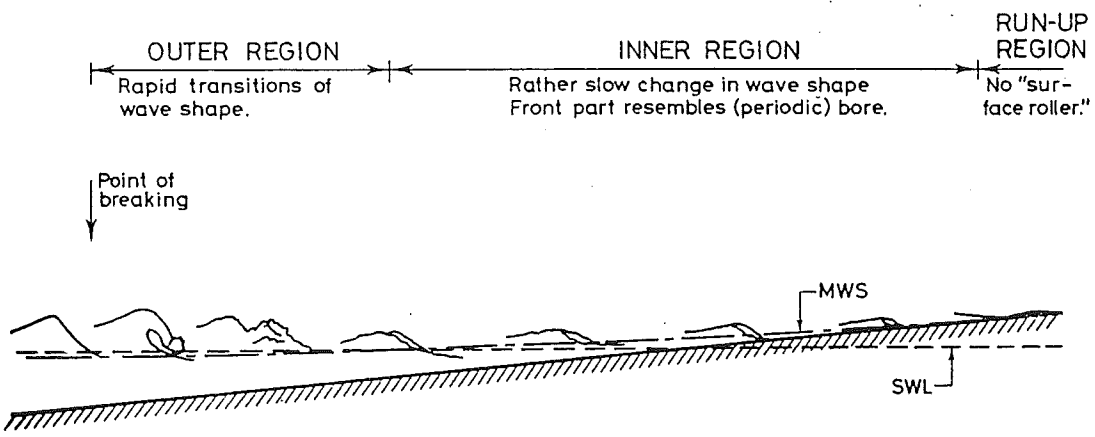

Figure 3: A schematic description of the wave characteristics in the surf zone [from Svendsen *et al.* (1978)].

3 The Short-Wave Motion

3.1 Introduction

In this section we review our present understanding of surf zone waves. Till recently, our understanding of surf zone waves was entirely qualitative and limited to describing patterns observed in laboratory and field experiments. These are reviewed in Section 3.2. As seen from the equations derived in the previous section, predictions of short-wave-averaged motions in the surf zone require information about the integral quantities associated with surf zone waves. Theoretical and empirical results for these quantities are discussed in Section 3.3. The turbulence generated by the breaking undoubtedly plays a crucial role in the dynamics of the surf zone, and this topic is reviewed in Section 3.4. Finally, recent contributions to modelling breaking waves in the time domain are discussed in Section 3.5.

3.2 Qualitative Description

Figure 3 shows a schematic of the wave motion from the breaker point to the shoreline of a gently sloping beach as most littoral beaches are. The way in which the waves break depends on the wave characteristics (deep-water wave height, wave period) and the bottom slope. The patterns range from the relatively controlled "spilling" to the violent and relatively sudden "plunging" breaker type (Galvin 1968, 1972).

In any type of breaking, there will be a rapid and substantial change in the shape of the wave immediately following the initiation of breaking. This happens over a relatively short distance

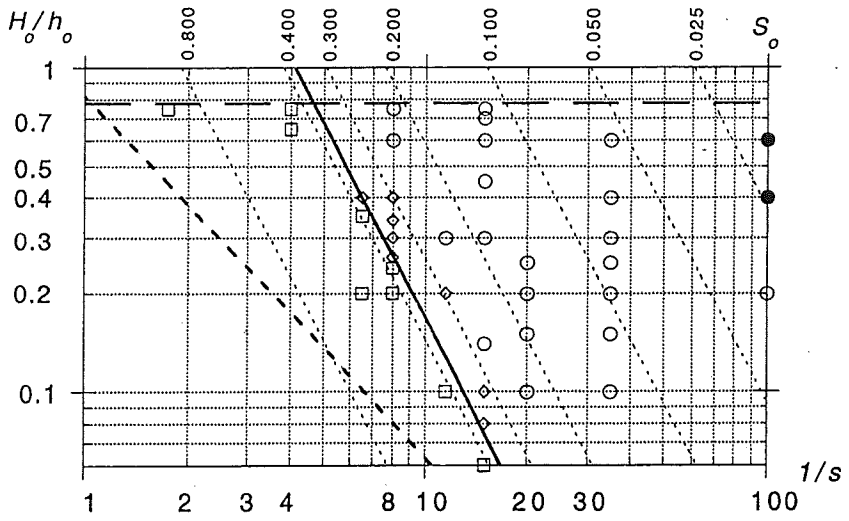

Figure 4: Empirical breaking criterion for solitary waves on a plane slope (full line). s is the bottom slope, H_0 is the height of the wave generated at h_0. [from Grilli *et al.* (1994)].

of 8–10 water depths after the breaker point, and this region has been termed the "outer" or "transition region" (Svendsen *et al.*, 1978).

Shoreward of the transition region, the waves will change much more slowly. In this region, the broken waves have many features in common with bores. This is the so-called "inner" or "bore region" which stretches all the way to the shore (or, if the breaking occurred on a longshore bar, till the waves stop breaking by passing into the deeper water shoreward of the bar).

On many natural beaches, the foreshore is much steeper than the rest of the beach. In the run-up on the shore on such beaches (termed the swash zone), the wave motion often shows a different pattern from that of the rest of the surf zone. Here the waves sometimes turn into 'surging' breakers which represent the transition stage to no-breaking/full-reflection.

If the slope becomes sufficiently steep, the waves stop breaking and full reflection occurs. The slope at which this transition occurs has not been properly studied for periodic waves, but the breaking/reflection of solitary waves on uniform slopes has been studied intensively (Synolakis 1987, Synolakis & Skjelbreia, 1993, Grilli *et al.*, 1994). Synolakis (1987) provided experimental as well as analytical results based on Boussinesq theory. The very accurate computations for solitary waves using the Boundary Element Method (BEM) (Grilli *et al.* 1994) indicate that solitary waves break on a bottom slope h_x if the initial height H_0 of the wave satisfies the relation

$$\frac{H_o}{h_0} > 16.9 h_x^2 \tag{44}$$

where h_0 is the water depth in front of the slope. (44) is an empirical result based on the computations, and Figure 4 shows the results.

The Transition Region

The literature about the transition region is almost entirely descriptive and based on photo-

graphic and optical methods. Basco & Yamashita (1986) give an interpretation of the flow based on such information particularly for a plunging breaker and show how the overturning of the wave creates patterns that look chaotic but are nevertheless largely repeated from wave to wave. Similar interpretations are given by Tallent *et al.* (1989). Janssen (1986) has mapped the variation of the free surface in this region through high speed video recordings of fluorescent tracers. Finally, Okayasu (1989) gives detailed measurements of the entire velocity field in the transition region from experiments using laser doppler velocimetry. The results have been obtained by repeating the same experiments many times and each time averaging over several waves and therefore cannot quite be regarded as a picture of the instantaneous velocity field in a particular wave.

The Bore Region

In the bore region, the information about the wave properties is also almost entirely empirical. It is only recently that predictive models of the actual wave motion have started to appear in the literature, and so far they can only predict the wave surface profiles. These models are discussed further in Section 3.5.

Knowledge about the waves in this region is far more quantative, however, than for the outer region. Among the experimental results for the bore region, it can be mentioned that Svendsen *et al.* (1978) found that the wave surface profiles develops a relatively steep front with a much more gently sloping rear side. The shape of the rear side of the wave will change from a concave towards an almost linear variation as the waves propagate shoreward while continuing to break so that near the shore of a gently sloping beach the wave is close to a sawtooth shape. Figure 5 shows the tendency.

Measurements of velocity fields using laser doppler velocimetry in propagating waves have been reported by Stive (1980), Stive & Wind (1982), Nadaoka & Kondoh (1982), Nadaoka (1986), and Okayasu (1989). In all cases, however, the measurements are limited to the regions away from the crest because none of the measuring techniques available today make it possible to measure velocities in the highly aerated region near the front of the breaker. That means that wave-averaged quantities such as radiation stresses, S_r, and energy flux, E_f, which get significant contributions from those regions, can only be determined with limited accuracy on the basis of such measurements. Stive & Wind (1982) give a detailed account of the problem. A further discussion of the available results is given in the following subsection.

3.3 Theoretical and Empirical Data for Surf Zone Waves

In most cases, linear (or "sine") wave theory has been used to calculate the wave-averaged quantities also inside the surf zone in spite of the fact that the breaking waves are far from sinusoidal in shape and are also not of small amplitude. The wave model used by Svendsen (1984a) acknowledges that surf zone waves are non-sinusoidal, long waves (length $\gg$ depth) and especially accounts for the fact that in breakers a volume of water (the surface roller) is carried with the wave at speed c. The situation is illustrated in Fig. 6.

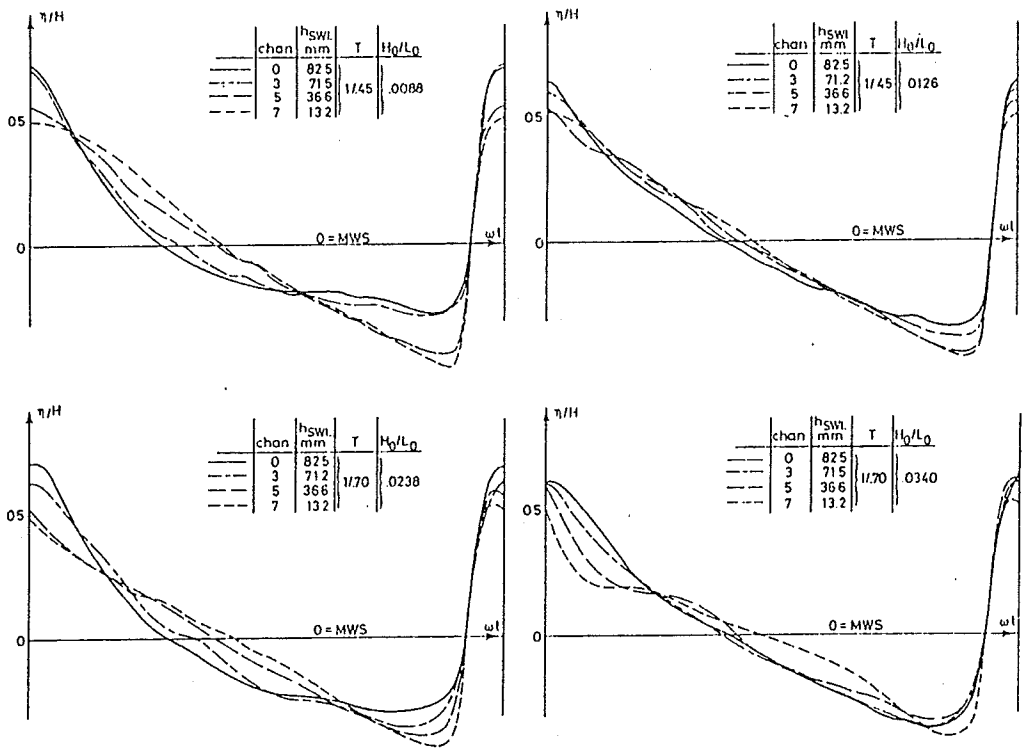

Figure 5: The development of wave profiles in the surf zone [from Svendsen *et al.* (1978)].

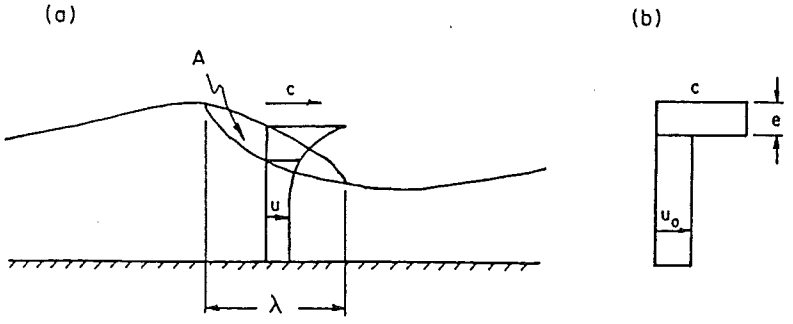

Figure 6: An assumed vertical variation of the horizontal velocity in surf zone waves [from Svendsen (1984a)]. Note that in this model the effect of the 'roller' is incorporated by assuming that the roller is carried with the wave speed, c.

Using these assumptions, it is found that in the wave direction the radiation stress is given by

$$S_r = S_m + S_p \tag{45}$$

where

$$S_m = \rho\, g\, H^2 \left(B_0 + \frac{A}{H^2}\,\frac{c}{gT} \right) \tag{46}$$

$$S_p = \frac{1}{2}\,\rho\, g\, H^2\, B_0 \tag{47}$$

$$E_f = \rho\, g\, c\, H^2 \left(B_0 + \frac{1}{2}\,\frac{A}{H^2}\,\frac{c}{gT} \right) \tag{48}$$

B_0 defined as

$$B_0 = \frac{\overline{\eta^2}}{H^2} \tag{49}$$

A is the area of the surface roller in the vertical plane. A was measured by Duncan (1981), and Svendsen (1984a) found the approximation $A/H^2 = 0.9$ constant over the surf zone based on Duncan's data. Later, Okayasu (1989) suggested that a more accurate expression may be $A/HL = 0.06$.

The energy dissipation due to breaking is often assumed equal to the dissipation in a hydraulic jump or bore of height H. This was first suggested by LeMehaute (1962), and has been widely used since then (*e.g.*, Miller & Barcilon 1978, Thornton & Guza 1983, Svendsen 1984a; Battjes and Janssen (1978) used it in an approximate form). Then the dimensionless dissipation D becomes

$$D = D_{\text{bore}} = \frac{h^2}{d_t\, d_c} \tag{50}$$

where d_t and d_c are the depths under the wave trough and wave crest, respectively (Svendsen *et al.*, 1978). It turns out that this relationship can be expressed in terms of the wave height to water depth ratio $\frac{H}{h}$ and the ratio η_c/H where η_c is the crest elevation. For most surf zone waves (50) gives values of $D_{\text{bore}} \sim 0.9$ (Svendsen, 1984a).

Thus the characteristics of the wave motion used as parameters in this theory (in addition to A) are B_0, the wave phase velocity c, and η_c/H. For sine waves, $B_0 = 1/8 = 0.125$ and $\eta_c/H = 0.5$. However, all of these are physical quantities that can be measured fairly easily. Hansen (1990) analyzed original data from most of the detailed laboratory experiments available and developed empirical representations for those parameters that, in most cases, fit the data remarkably well.

Dally *et al.* (1985) observed that if the ratio of wave height to water depth decreases below a certain level (roughly between 0.35 and 0.40) real waves will stop breaking. They therefore asssumed that the energy dissipation at any point is given by

$$D = \frac{-K}{h}(Ec_g - (Ec_g)_s) \tag{51}$$

where K is a dimensionless decay coefficient. The value of $(Ec_g)_s$ is chosen so that the dissipation D becomes zero when the wave height H decreases to or below approximately 0.40 times the water depth. This approach is particularly realistic on beaches with bars or shoals where the ratio of wave height to water depth may decrease below the threshold when the waves propagate from shallower into deeper water, e.g., shoreward of a bar.

Empirical Results for Surf Zone Waves

As discussed previously, a satisfactory wave theory does not exist for surf zone waves. In consequence, almost all of our knowledge about surf zone waves comes from analyzing observations of breaking waves. Presently, empirical results are available for the wave celerity and some of the integral quantities (radiation stress, energy flux, and rate of energy dissipation). These results are briefly discussed below. Clearly, an accurate estimation of these quantities is crucial for proper quantitative modeling of surf zone circulations.

The celerity of surf zone waves has been analyzed by Svendsen *et al.* (1978) and Thornton & Guza (1982). Svendsen *et al.* analyzed the celerity of regular waves in a laboratory and found it to be somewhat higher than the shallow-water prediction ($c = \sqrt{gh}$). Thornton & Guza measured the wave celerity in a natural surf zone. They showed that well offshore of the surf zone (in 7m water depth) the measured speed agreed well with the predictions of linear wave theory. Inshore of this location, however, they found marked discrepancies between the measurements and linear theory predictions. In particular, they found that in the surf zone and just offshore the wave celerities showed weak amplitude dispersion and almost no frequency dispersion.

The energy dissipation in breaking waves has been analyzed by Svendsen *et al.* (1978) and Stive (1984). Both studies found that the energy dissipation in breaking waves is somewhat higher than that in a bore.

Recently, Svendsen & Putrevu (1993) analyzed a number of laboratory measurements to determine the variation of thenondimensional radiation stress (P), energy flux (B), and energy dissipation (D) inside the surf zone. As an example, Figure 7 shows results for the dimensionless radiation stress P for different relative bottom slopes represented by

$$S_B = \left(\frac{h_x L}{h}\right)_B \tag{52}$$

the value at the breaking point of the slope parameter mentioned earlier. h_x is the bottom slope (constant) in the experiments, $L = cT$ the wave length, and h_B the water depth at breaking. Also shown (for comparison), in Figures 7 is the P value of 1/8 corresponding to the linear long wave theory.

Several conclusions were drawn from the results presented by Svendsen & Putrevu:

1. First, the (not very surprising) conclusion that sine wave theory is inappropriate as approximation for P (and hence B).

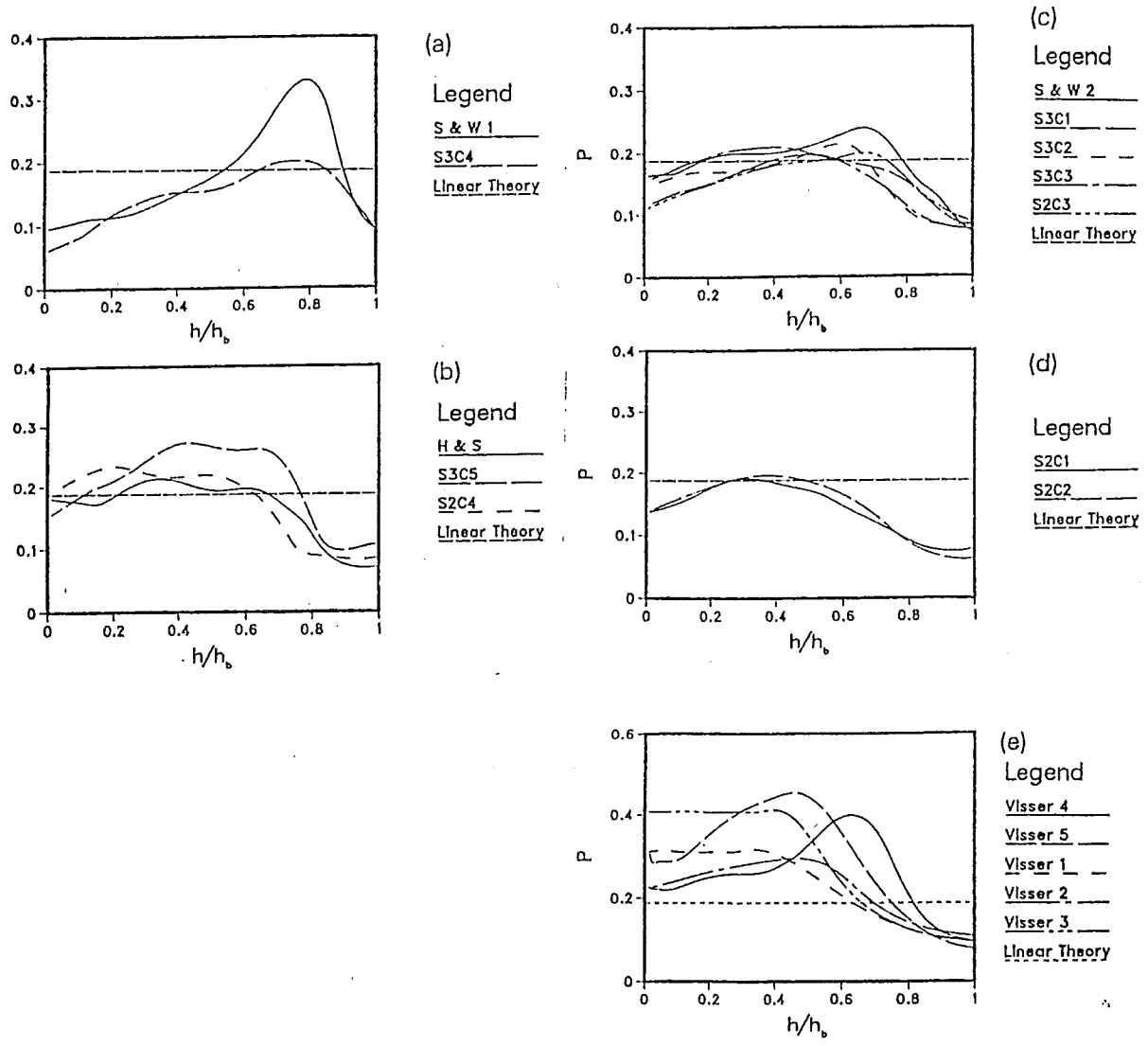

Figure 7: Empirically determined cross-shore variations of the nondimensional radiation stress P [from Svendsen & Putrevu (1993)]. The solid line in these figures represents the predictions of linear long wave theory. curves marked S & W are based on the experiments by Stive & Wind (1982), the curves marked SxCx on are based on the experiments of Okayasu (1989), H & S is Hansen & Svendsen (1984), and Visser x is experiment x from Visser (1982). The first four figures represent four intervals of values for S_b namely: a) $S_b < 0.4$, b) $0.4 < S_b < 0.5$, c) $0.5 < S_b < 0.85$, d) $0.85 > S_b$.

2. Though the variation of the wave properties such as radiation stress, $S_{\alpha\beta}$, and energy flux, $E_{f,\alpha}$, clearly depend on the variation of the wave height (the most important parameter), the variation of the wave shape represented by P (and B) is also important for the correct prediction of radiation stress and energy flux.

3. If the breaking were almost equal to that in a bore, we would have $D \sim D_{\text{bore}}$, that is, $D \sim 1$. In most cases, the actual dissipation is substantially larger (from 50% to several hundred percent).

The Surf Similarity Parameter

The empirical results for the short-wave-averaged quantities were presented above in terms of the beach slope parameter S (introduced in Section 1). An alternative parameter, the so called Surf Similarity parameter ξ, has also been frequently used in the surf zone. It is defined as

$$\xi = \frac{h_x}{\sqrt{H/L_0}} \tag{53}$$

where L_0 is the linear deep water wave length. This parameter was first introduced by Irribarren & Nogales (1949), and the derivation modified by Battjes (1974). The name of this parameter is somewhat misleading, however, because it is derived on the basis of a situation with standing (rather than breaking) waves on a steep beach with full reflection, and it is (somewhat heuristically it seems) assumed that the (standing) waves break at the first node from the shoreline. The depth at that node is then used as a characteristic depth which is used to determine the breaking wave height.

It is evident that this situation has little resemblance with the wave motion in an actual surf zone where waves are propagating and breaking at a depth which is more a function of what happens seaward of the breaking point than of the distance to the shore. It is therefore surprising that this parameter has been so widely successful in classifying surf zone conditions. It may partly be due to the fact, that on a plane beach it has been shown that a special version of the Surf Similarity parameter $\xi_0 = \frac{h_x}{\sqrt{H_0/L_0}}$ is related to S_b – the value of the Beach Slope parameter at the breaking point – by the expression

$$S_b = 2.30\xi_0 \tag{54}$$

(Svendsen, 1987). Thus, since H at the break point is often close to H_0, evaluating ξ closely corresponds to evaluating the (more appropriate) parameter S_b. This could be part of the reason for the meaningful results obtained using ξ.

Whereas S_b may be the appropriate sustitute for ξ, the general parameter S has another advantage in addition to being based on assumptions closely related to actual surf zone conditions: it is a local parameter, defined at each point in the surf zone. Hence it can describe the situations on arbitrary beach profiles.

Thus, in the present paper we have decided to use S and S_b as surf zone parameters.

3.4 Breaker-Generated Turbulence

Turbulence

In a surf zone wave the separation of measured velocities into "wave" and "turbulent" components is not straightforward. In steady flows, the turbulent component of the velocity is usually defined using an ensemble-averaging procedure. In principle, an analogous procedure could be used to define the turbulent component in monochromatic surf zone waves – averaging the velocity from the same phase from successive waves would lead to a quantity equivalent to an ensemble average. However, this method is far from being trivial. It turns out that even in well controlled laboratory experiments the wave period of initially monochromatic waves does not remain constant as the waves propagate in the surf zone. This makes the identification of the phase of the wave motion problematic. As can be easily appreciated, the situation is far more complicated in a natural surf zone where the waves are irregular. A completely satisfactory method of separating the velocity in surf zone waves into "wave" and "turbulent" components has not been developed yet. It is important to keep this in mind while considering the results described below.

Peregrine and Svendsen (1978) found experimentally that the turbulence generated by the breaking, while initiated at the toe of the turbulent wave front, spreads downwards and continues to do so long after the breaker has passed. They speculated that the spreading mechanism is similar to that in a shear layer. Battjes & Sakai (1981) presented LDV measurements for the velocity field underneath the breaker generated by a hydrofoil positioned some distance below the water surface in a steady current. Their results for the rate of variation of the turbulence indicated that the flow has more similarities to the flow in a wake. The truth is probably that the turbulence generated by wave breaking and its dispersion is different from all other turbulent phenomena.

Measurements in a steady breaker behind a hydrofoil were also made by Duncan (1981) who used photographic techniques to detemine the extent of the roller, which is the recirculating mass of water created by the highly turbulent flow down the front of the slope of the breaker. Lately, Lin & Rockwell (1994) have used the technique of Particle Image Velocimetry (PIV) to determine the entire velocity field beneath a similar breaker. They also obtained information about the vorticity field which shows that the maximum vorticity occurs in a region positioned approximately where we would expect to find the dividing steamline to the surface roller. Above that (in the 'roller'), the vorticity is very weak. They concluded that the instantaneous velocity fields do not show clear signs of a vortex type of surface roller (though the present authors seem to find indications of such a roller in Fig. 2a in the paper). It is obvious, however, that the strong turbulent fluctuations totally dominate over the weak mean flow in the roller region, and hence the roller structure can only be expected to show up in the picture of the mean velocity field.

For completeness it is noted that not too far from the free surface the velocities under hydrofoil-generated breakers used by Battjes & Sakai (1981) and Lin & Rockwell (1994) will probably closely resemble those in a (deep water) breaking wave, whereas at some distance farther down from the surface the flow is likely to be disturbed by the flow around the hydrofoil and hence be quite

different from at least what we find in a surf zone breaker.

Laboratory measurements of the distribution of turbulent intensities below the MWL in periodic waves were reported by Stive & Wind (1982), Nadaoka & Kondoh (1982), Nadaoka (1986), and in more detail by Okayasu (1989) and Ting & Kirby (1994). Thornton (1979) and George *et al.* (1994) reported similar measurements in the field.

Data for breaker-generated turbulence has also been provided by Hattori & Aono (1985) who found that the turbulent energy spectra have large proportions of the energy at frequencies only somewhat higher than the wave frequency indicating the existence of large scale vortices. Nadaoka (1986) and Nadaoka *et al.* (1989) identified a regular system of vortices with axes sloping downwards from the free surface and developing at some distance behind the front.

Battjes (1975) and later Svendsen (1987) analyzed turbulent kinetic energies under breaking waves. Battjes analysed the value of the eddy viscosity under breaking waves based on the assumption that $\nu_t = l\sqrt{k}$ and related k, the turbulent kinetic energy, to the energy dissipated in the breaking process. Svendsen found that most of the energy is actually dissipated in the crest above the MWL. George *et al.* (1994) analysed data from field experiments and compared the results for the turbulence intensities with the laboratory data. They found that while the intensity of the turbulence in the field was reduced relative to laboratory data, the characteristics of the turbulence remain the same.

The details of the highly turbulent area at the front (the so-called "roller") were analyzed by Longuet-Higgins & Turner (1974) who assumed that air entrainment played a vital part in maintaining this roller in position on the sloping front. Later results of experiments by Duncan (1981), and analysis such as Svendsen & Madsen (1984), Banner (1987, and Deigaard & Fredsoe (1989) all in various ways attribute the support of the roller to turbulent shear stresses. Longuet-Higgins (1973) also analyzed the nature of the flow in the neighborhood of the toe of the roller assuming a separation point here. An alternative flow pattern with a singularity in the vertical velocity gradient at the toe but continuity in the shear stress was used in the model developed by Svendsen & Madsen (1984).

3.5 Time-Domain Models

Time-domain models are models that essentially solve the hydrodynamical equations in a form that can include the process of wave breaking and hence provide information about the phase motion. Several such models are presently in use and they are discussed below on the basis of the basic approximation used to derive the underlying equations. They are all based on long-wave assumptions such as the Nonlinear Shallow-Water (NSW) equations or Boussinesq equations, and it has become increasingly evident that these representations are much more accurate than the nature of the underlying assumptions would lead us to believe.

Nonlinear Shallow-Water Equation Models

The nonlinear shallow-water equations are based on the assumption that the characteristic horizontal scale λ is large in comparison to the water depth h (i.e., $\mu = \frac{h}{\lambda} \ll 1$) and the wave amplitude to depth ratio $\delta = H/h$ is of order one. In Boussinesq terms, this means that the Ursell parameter $U_r = \frac{\delta}{\mu^2} = \frac{H\lambda^2}{h^3}$ is much larger than one. This leads to equations that correspond to the linear shallow-water equations (equivalent to the mild-slope equation) with additional nonlinear terms even in the first approximation. It also follows from the mentioned scale assumptions that in that approximation the pressure is hydrostatic and the horizontal velocity is uniform over depth.

This leads to the following equations which essentially are the equations for conservation of mass and momentum

$$\frac{\partial \zeta}{\partial t} + \nabla_h(\mathbf{u}(h+\zeta)) = 0 \tag{55}$$

$$\frac{\partial \mathbf{u}}{\partial t} + \mathbf{u}\nabla_h\mathbf{u} + g\nabla_h\zeta = 0 \tag{56}$$

where $\mathbf{u}$ represents the (depth uniform) horizontal velocity vector and ∇_h is the horizontal gradient operator. Notice that in (56) the bottom friction, represented by the friction factor f, can be included by replacing the zero on the right hand side of (56) by the term $-\frac{1}{2}\frac{f}{h}|\mathbf{u}|\mathbf{u}$.

If we disregard the bottom friction term (which is small) these equations conserve mass and momentum and they include no terms that represent the dissipation of energy at wave breaking. Hence, an exact solution to (55) and (56) will also conserve energy. Due to the lack of frequency-dispersion mechanisms, they also do not have solutions of constant form: any initial wave, no matter how small, will steepen on its front side as it propagates and eventually the front will become vertical as if the wave were breaking. At that point, however, the underlying assumptions of course break down because the characteristic horizontal length (the length from trough to crest, say) is no longer large in comparison to the water depth.

The use of these equations to describe breaking waves is then based on the fact that if solved numerically by means of a Lax-Wendroff (or similar dissipative) scheme artificial dissipation is introduced in such a way that the steepening of the front of the wave stops just before the front becomes vertical. We then have a permanent-form long wave of finite amplitude for which mass and momentum are conserved and it can be shown, by methods similar to the analysis of a hydraulic jump, that in such a wave energy is dissipated. On a constant depth with no change in wave form the dissipation will then equal the dissipation in a bore of the same height (Svendsen *et al.*, 1978) (hence the relevance of the assumption that the energy dissipation in the short-wave averaged energy equation is equal to that in a bore, see Section 3.3).

This method for describing breaking waves has been developed extensively in the past fifteen years, starting with Hibberd & Peregrine (1979), followed by Packwood & Peregrine (1980) and Packwood (1983) which particularly discussed the effect that the porous bed on sandy beaches has on the final stages of the runup process. Watson & Peregrine (1992), Watson *et al.* (1992), Barnes *et al.* (1994) have continued the exploration of the wave propagation using an alternative numerical method for the solution.

Other details of the wave motion such as surface profile, particle velocities, set-up etc. have

also been analysed using the NSW equations from just before the onset of breaking by Kobayashi and co-workers who first developed the computer program IBREAK (Kobayashi *et al.*, 1989) and later the improved version RBREAK (Kobayashi & Wurjanto, 1992). They have particularly explored the benefits of the method in the swash zone where the bottom slope is steep. This is particularly useful because under those conditions the motion is poorly covered by gentle slope assumption underlying the wave averaged models. Much of their work deals with the steep slopes of engineering structures.

The strengths of this method include the following:

1. The method is relatively simple and robust, though the time step in the integration process needs to be kept small enough to keep the Courant-number less than one. This becomes a practical problem where the water depth is small as in the runup.

2. Being a time-domain model, it is also capable of describing the temporal development of random wave motion (see, *e.g.*, Kobayashi & Wurjanto, 1992; Cox *et al.*, 1992, 1994). It also is not restricted to a plane beach (see the same references).

3. Properly used the results such as wave surface profiles and wave heights have remarkably close resemblance with observations in particular in the swash zone (Cox *et al.* 1992, 1994).

4. So far these models have only been used in one-dimensional cross-shore computations. However, the equations (55, 56) apply to two horizontal directions and hence can in principle describe situations with obliquely incident waves and longshore variations in the topography. With appropriate boundary conditions, the model should also be able to reproduce net flows in the swash zone such as currents and long-wave motion at least with some accuracy. There would be some doubt, though, as to the capability of these equations to correctly model the part of the radiation stress originating from the front of the breaking waves because the fronts are not accurately modelled by these equations (see below).

The weaknesses of this method are the following:

1. Since the model does not contain the mechanism that, in nature, balances the nonlinearity and resists the wave steepening (such as non-hydrostatic pressure), it cannot predict the onset of breaking. The position of breaking is determined by the distance from the offshore boundary of the computation: the waves will break a certain distance from that boundary. Hence the position of the offshore boundary needs to be chosen so that the model reproduces the "correct" (known) breaking point. For irregular waves, that may not always be possible for all waves in the time series.

2. The front steepens until a certain point where the (numerical) dissipation is large enough and then remains frozen. The steepness of the front in that situation corresponds to a few times dx. Hence the actual form of the front is not represented by the model but depends on the choice of discretization length.

3. Having a depth-uniform velocity, the model only reproduces the depth-averaged velocity in the waves. (See point 4 above.)

Boussinesq Models

In recent years models based on Boussinesq approximations [$U_r = O(1)$] have been extended to describe conditions similar to breaking waves. The first of these models was based on simply adding a dissipation term to the momentum equation in the Boussinesq model. Thus Karambas *et al.* (1990) solve the equations

$$\frac{\partial \zeta}{\partial t} + \frac{\partial}{\partial x}\left((h+\zeta)\,\tilde{u}\right) = 0 \tag{57}$$

$$\frac{\partial \tilde{u}}{\partial t} + \tilde{u}\frac{\partial \tilde{u}}{\partial x} + g\frac{\partial \zeta}{\partial t} - \frac{h}{2}\,\frac{\partial^3 (h\tilde{u})}{\partial t \partial x^2} + \frac{h}{6}\,\frac{\partial^3 \tilde{u}}{\partial t \partial x^2} + g\frac{\tilde{u}\mid \tilde{u}\mid}{C^2\,(h+\zeta)} - \nu_t \frac{\partial^2 \tilde{u}}{\partial x^2} = 0 \tag{58}$$

in which a bottom friction term represented by the Chezy coefficient C has also been included. $\tilde{u}$ is the depth-averaged velocity; ν_t, an eddy viscosity. (See also Karambas & Koutitas (1992)).

Zelt (1991) essentially solved the same equations but on Lagrangian form and focused on the runup of the solitary waves. The cases with wave breaking were surging or collapsing breakers and he found that the agreement with measurements of the surface profiles of the waves was quite good though obviously the Boussinesq assumptions are not satisfied when the front of the actual wave turns vertical.

A somewhat different approach was used by Brocchini *et al.* (1992) and by Schäffer *et al.* (1992, 1993). Both these models include the effect of the surface roller in the breaking waves.

Brocchini *et al.* used the Serre equations. These equations represent the next order of approximation [to $O(\mu^2)$] from the NSW equations in terms of the long-wave parameter μ. Hence they include the same dispersive terms as ordinary Boussinesq waves but assume the Ursell parameter $U_r \gg 1$. Brocchini *et al.* focused on the effect that the roller has on the frequency dispersion term.

Schäffer *et al.*, on the other hand, only included the effect of the roller in the nonlinear term. They solve the depth integrated form of the Boussinsq equations

$$\frac{\partial \zeta}{\partial t} + \frac{\partial Q}{\partial x} = 0 \tag{59}$$

$$\frac{\partial Q}{\partial t} + \frac{\partial}{\partial x}\left(\frac{Q^2}{h}\right) + \frac{\partial R}{\partial x} + gh\frac{\partial \zeta}{\partial x} + \frac{h^3}{6}\,\frac{\partial^3}{\partial x^2 \partial t}\left(\frac{Q}{h}\right) - \frac{h^2}{2}\,\frac{\partial^3 Q}{\partial x^2 \partial t} = 0 \tag{60}$$

where Q is the depth-integrated horizontal velocity and the R term represents the only explicit effect of the surface roller. Implicit effects are included in Q, however. R is calculated from a heuristically assumed velocity distribution, which includes a representation of the roller.

The results of all these models show that waves become skew and decrease in height as it is seen in the surf zone. In the first type of the models, however, the effect is achieved by including a dissipation term that essentially originates from the horizontal component of the turbulent normal stresses. This term is usually considered a small contribution to the momentum balance. The other two models (Brocchini *et al.* and Schäffer *et al.*) each use different assumptions to incorporate the roller effect. This seems likely to be the dominating effect that wave breaking has on the momentum balance. In contrast to the NSW models, the Boussinesq waves are stable and will never develop a vertical front because, as the wave height increases towards the breaking height, the crest steepens, and at this stage of the process all Boussinesq models overestimate the dispersive effects of the surface curvature. This overstabilizes the wave and prevents vertical fronts from developing in the model. Hence it applies to these models as well that they actually cannot predict the point at which the waves are breaking. It must be specified (*e.g.*, from the shape of the wave surface profile in combination with empirical information). The velocity profiles are quadratic in the vertical coordinate. Though this is clearly a much better approximation to the actual velocity variation in waves than the depth-uniform velocity in the NSW equations, it still falls short of predicting the sharp increase in the velocity near the crest of a breaking wave (van Dorn 1976, Grilli *et al.* 1994).

4 Bottom Boundary Layers and Shear Stresses

Near the bed a boundary layer develops which gives rise to bottom shear stresses and locally generated turbulance.

The Bottom Shear Stress

Since the current velocity usually is weaker than the velocity amplitude in the wave motion, this boundary layer is essentially oscillatory in nature and its thickness is small in comparison to the water depth.

Under non-breaking waves, it is important to understand the mechanisms behind generation and diffusion of turbulence in the wave-current flow above the boundary layer because this significantly influences the current motion. In breaking waves, however, the turbulence generated in the bottom boundary layer only dominates inside that boundary layer. In the water column above the boundary layer, by far the dominating source of turbulence is the wave breaking, and the turbulence spreads downwards from the surface usually within one wave period or less rather than diffusing upwards from the bottom (see section 3.4).

As a consequence of the structure of this flow, the bottom boundary layer can be expected primarily to exercise influence on the flow in the main part of the water column through the effect of the bottom shear stress. This has particular bearing on the depth-integrated, short-wave-averaged models as well as time domain models as the equations show [see, e.g., (13) and (56)]. Hence in such models we only need to establish a relationship between the mean bottom shear stress $\overline{\tau_\alpha^B}$ and the current outside the boundary layer. Conversely, the current and wave velocities and pressure gradients determined by such models will act as forcing for the boundary layer flow.

Several such relationships have been developed through the solutions described below for the boundary layer flow. However, a practical approach introduced by Longuet-Higgins (1970) has been to assume that the instantaneous shear stress $\tau_\alpha^B(t)$ can be expressed in terms of a friction factor f by a relation of the form

$$\tau_\alpha^B = \frac{1}{2}\,\rho\, f\, [V_\alpha + u_{w\alpha}(t)|V_\alpha + u_{w\alpha}(t)|] \tag{61}$$

which can be considered a generalization of the relationship for the maximum shear stress introduced by Jonsson (1966). [Note that the summation rule does not apply to (64) because $|V_\alpha + u_{w\alpha}(t)|$ is a scalar]. For weak currents and waves nearly perpendicular to the currents, this can (after time averaging) be simplified to the following expression for the short wave averaged shear stress τ_α^B

$$\tau_\alpha^B = \frac{1}{\pi}\,\rho\, f\, u_o\, V_\alpha \tag{62}$$

where u_o is the bottom velocity amplitude in the waves. Liu & Dalrymple (1978) studied various other cases of $\overline{\tau_\alpha^B}$ derived from (61) such as strong currents relative to the wave motion, and

Svendsen and Putrevu (1990) showed that in general $\overline{\tau_\alpha^B}$ obtained from (61) can be written

$$\overline{\tau_\alpha^B} = \frac{1}{2}\,\rho\, f\, u_o \{V_\alpha\, \beta_1 + u_{o\alpha}\, \beta_2\} \tag{63}$$

where β_1 and β_2 are functions of $u_o = |u_{o\alpha}|$ and $V_b = |V_\alpha|$ and of the angle μ between the wave and the current directions. The variable $u_{o\alpha}$ is the amplitude of the wave particle motion

The Bottom Boundary Layer

The motion is almost always a combination of a wave and a current motion so analysis of the boundary layer flow needs to include the effect of the current. Analytical theories for wave-current interactions in bottom boundary layers have been developed by Grant & Madsen (1979), Trowbridge & Madsen (1984), Fredsoe (1983), Christoffersen & Jonsson (1985), Davies *et al.* (1988), all for essentially non-breaking wave conditions which first of all means sinusoidal or second order Stokes waves. Schäffer & Svendsen (1986) analyzed the effect of breaker-like wave motion represented by a sawtooth time profile for the velocity above the boundary layer.

There are also numerical solutions of the boundary layer equations using one and two equation turbulent closure models. These, however, are to the authors' konwledge for situations with non-breaking waves and are therefore not included here.

One of the questions that have been raised (Svendsen *et al.* 1987) is whether in fact the vortices of the breaker induced turbulence reaching the bottom may be strong enough and of sufficiently large scale to momentarily and locally wash away the entire bottom boundary layer.

Although very important, the details of the bottom boundary layer flow is one of the topics that we have, due to space limitations, left out of this review.

5 Nearshore Circulation, Short-Wave-Averaged Models

5.1 Introduction

In the present section we briefly review some of the problems studied in the past 20 years. These problems have been studied using short-wave-averaged modelling, and we review the progress made in the development of these models. At the same time, the steady nearshore circulation has also been subject to substantial analysis on the basis of laboratory and, particularly, field measurements, and some of these efforts are reviewed as well in this section.

5.2 Recent Advances in Steady Circulations

The Cross-Shore Wave Height and Set-up Variation

As shown in Section 3, the short-wave-averaged quantities (radiation stresses, energy flux, etc.) are proportional to the square of the wave height. Briefly one can say that in short-wave-averaged models, solution of the energy equation will supply information of the variation of the wave height, H, and hence the mass flux and radiation stress forcing, whereas solution of the continuity and momentum equations will provide information about water level variations $\overline{\zeta}$ and currents V_α induced by this forcing. Therefore, the prediction of the wave height, in particular inside the surf zone, is important for a successful modelling of all the wave-generated nearshore phenomena. As also mentioned earlier, this prediction is closely linked to the correct assessment of the nondimensional parameters P for radiation stress and D for the energy dissipation due to breaking. This problem was addressed in Section 3.4. With these parameters known, the wave height follows from the energy equation.

The simplest possible approach, however, is to utilize the observation that on a gently sloping beach the waves break due to the decreasing water depth maintaining an almost constant ratio between breaking wave height and local water depth (Munk 1949a). Thus, by this approach, the surf zone wave height is determined as

$$H = \gamma h \tag{64}$$

where γ is assumed constant. Essentially (64) replaces the energy equation (26). This assumption has been used extensively and can, in many cases, be justified by the fact that it gives qualitatively the correct type of variation of the wave height. Examples that use (64) include the first paper determining the variation of setup, $\overline{\zeta}$, in the surf zone (Bowen *et al.* 1968) and the first papers dealing with the cross-shore distribution of longshore currents (Bowen 1969a, Thornton 1970, Longuet-Higgins 1970).

The simplifying assumption (64), however, is at variance with the fact that, at a closer look, the ratio of wave height to water depth in the surf zone is not constant. This was already discovered experimentally by Horikawa & Kuo (1966). They showed that not only does the ratio

decrease from an initial maximum at the breaking point but the experiments also suggested that on a plane beach this ratio may reach a minimum near the shoreline and then increase again.

The first complete solution of the cross-shore variation of wave height and setup in which the energy equation was solved together with the cross-shore momentum equation instead of using (64) was given by Hwang & Divoky (1970). They used cnoidal wave theory for the short-wave-averaged quantities in the surf zone. Later, by evaluating the short wave averaged parameters in the energy and momentum equations by the method described in Section 3.3, Svendsen (1984a) confirmed the existence of a minimum for the wave height to water depth ratio. It turns out that by simply sustituting the the definitions for B and D into the energy equation (26) and rearranging the terms this equation can be written as the following equation for the wave height to water depth ratio (Svendsen *et al.*, 1978)

$$\left(\frac{H}{h}\right)_x = -\left(\frac{h_x}{h} + \frac{c_x}{2c} + \frac{B_x}{2B}\right)\frac{H}{h} + \frac{D}{8LB}\left(\frac{H}{h}\right)^2 \tag{65}$$

where index x represents differentiation with respect to x. Since the only assumption used to derive this equation from (26) is that the waves are periodic, this equation is well suited to identify the various mechanisms that determine wave height variation, in particular in the surf zone. The first parenthesis on the right hand side represents the shoaling effect due to the variations in water depth which, in addition to the direct h_x-term, comes in through the change in phase velocity c and in the wave shape represented by B. The second parenthesis represents the energy dissipation (or gain through, say, wind generation if D is assumed > 0). It is evident from the fact that the energy term is proportional to $\left(\frac{H}{h}\right)^2$ that as the value of $\frac{H}{h}$ decreases through the surf zone the shoaling mechanism (first parenthesis) may begin to dominate which causes the above mentioned minimum in $\frac{H}{h}$. It also turns out that if B and D are independent of $\frac{H}{h}$ then (65) is a Bernoulli equation which can be solved analytically (Svendsen, 1984a).

One of the observations made by Svendsen (1984a) was that, in spite of the dramatic reduction in wave height that occurs shortly after breaking, the mean water level stays horizontal for quite a distance shoreward of the break point. The only possible explanation is that the radiation stress also stays constant which, using (43), can only happen if the shape of the wave changes so that P, the non-dimensional shape parameter in the radiation stress, increases in proportion to the decrease in H^2. This increase in P is reflected in the empirical results shown in Fig. 7.

In parallel with these efforts towards refining the accuracy of the prediction for regular waves, Battjes & Janssen (1978) developed the solution of energy and cross-shore momentum equations for a statistical description of random waves. In this work the wave height distribution is assumed to be a truncated Rayleigh distribution.

Battjes & Janssen also assume that at any given location a certain percentage of the waves are breaking. Offshore the percentage is zero, close to the shore 100% of the waves are breaking. Battjes & Stive (1985) calibrated this model using both laboratory and field data and showed that the model predicts the root-mean-square wave height well. The Battjes & Janssen model was refined by Thornton & Guza (1983). They analyzed field data for wave heights and showed

that the Rayleigh distribution describes the random wave height variation well throughout the nearshore region. Based on their observations, Thornton & Guza propose an empirical function for the distribution of breaking waves. Thornton & Guza also show that their model predicts both the root-mean-square wave height and the distribution well. The work on the transformations of random waves in the surf zone has been continued by Dally (1990, 1992) who only assumes that the waves are initially Rayleigh distributed and calculates the ensuing change in the distribution of the wave heights as they propagate shoreward and break. The method is based on the assumption that each wave represents an isolated event for which the local wave height causes a local energy dissipation and hence a reduction in the height of that particular wave. The percentage Q of waves that are breaking is one of the parameters of the model that is still being investigated.

At the present time, it is found that the wave-height-setup models are quite accurate for prediction of the wave height variation; in particular, such models that include empirical constants which have actually been calibrated to predict the experimental results for the wave height. The major inaccuracy usually occurs in the prediction of the setup, even if the delay after breaking is included artificially. The reason seems to be that the assumptions made about the value of P, the nondimensional radiation stress (in particular the use of sine wave theory), are too inaccurate. This is particularly unfortunate because, as (36) shows the radiation stress in any direction can be determined from the radiation stress of plane waves, and as (13) shows, the gradient of the general radiation stress is the major forcing for currents and infragravity motion in the surf-zone. Hence the inaccuracy of these models in predicting the cross-shore set-up on a simple, long straight coast really represents a similar inability to predict the proper forcing in general nearshore circulation problems (Svendsen & Putrevu, 1993).

Longshore Currents

The first solutions to the cross-shore variation of the longshore current pattern were given by Bowen (1969a), Thornton (1970), and Longuet-Higgins (1970). These early works clearly demonstrated that it was necessary to include lateral mixing to properly model the cross-shore distribution of longshore currents. As a result, much effort was devoted to understanding the mechanisms responsible for this mixing [early discussions may be found in Inman *et al.* (1971), Bowen and Inman (1974) and Battjes (1975)].

In most investigations, the mixing inside the surf zone was attributed to the strong turbulence generated by wave breaking in that region [see, *e.g.*, the discussion in Mei (1983), pp. 484-485]. The works of Bowen, Thornton, and Longuet-Higgins also suggested that it was necessary to assume a level of mixing outside the surf zone that was of the same order as the mixing inside the surf zone. However, no explanation was forthcoming for the source of the mixing outside the surf zone as observations (Harris *et al.* 1963, Inman *et al.* 1971, Nadaoka & Kondoh 1982) showed that the turbulence outside the surf zone was very weak.

Nearshore Mixing

In the field, the random nature of the incident wave field leads to a time variation of the point at which each individual wave is breaking. This corresponds to variations in the width

of the forcing region for longshore currents. Thornton & Guza (1986) demonstrated that these variations, when averaged over some time, provide an effect that is similar to mixing. They also demonstrated that when the time variation of the break point is taken into account, the additional smoothing of the longshore current profile, by including the turbulent mixing, is minor. Thus, Thornton & Guza suggest that the smoothing of the longshore current profile in the field may be due to the random nature of the incident wave field. While this mechanism is clearly important, it does not provide an explanation for the high level of mixing found in laboratory measurements of longshore currents generated by regular waves (*e.g.*, Visser 1984).

Oltman-Shay *et al.* (1989) identified temporal oscillations of longshore currents in the field. These oscillations (further discussed in Section 7) may be interpreted as a shear instability of the longshore current (Bowen & Holman, 1989). Such instabilities contribute a mixing mechanism which, under certain conditions, may be strong enough to account for the required mixing (Dodd & Thornton, 1990; Putrevu & Svendsen, 1992a; Church *et al.* 1994). However, theoretical estimates (Putrevu & Svendsen 1992a) as well as laboratory measurements (Reniers *et al.* 1994) suggest that it is unlikely that these instabilities develop under laboratory conditions involving plane beaches. Hence, they cannot account for the mixing observed in the laboratory experiments even though they clearly represent an important mechanism in the field.

Putrevu & Svendsen (1992b) and Svendsen & Putrevu (1994a) showed that the vertical nonuniformity of the current profiles leads to lateral mixing through a momentum dispersion mechanism. This mechanism is analogous to the dispersion of pollutants in a shear flow first discovered by Taylor (1954) and expanded on (among others) by Elder (1959) and Fischer (1978). Given below is a brief account of the mechanism considered by Svendsen & Putrevu.

On a long straight coast, the cross-shore distribution of alongshore uniform, steady longshore currents is governed by

$$\frac{d}{dx}\left(\int_{-h_0}^{\bar{\zeta}} UV\,dz + \overline{\int_{\zeta_t}^{\zeta} u_w V + v_w U\,dz}\right) + \frac{1}{\rho}\frac{d}{dx}\left[S_{xy} - \overline{\int_{-h_0}^{\zeta} \tau_{xy}\,dz}\right] + \tau_y^B = 0 \qquad (66)$$

In the above, U is the undertow, V is the longshore current, and τ_{xy} is the Reynolds' stress which is usually parameterized as

$$\tau_{xy} = \rho\nu_t \frac{dV_m}{dx} \qquad (67)$$

where V_m is the depth-averaged longshore current.

The first two terms in the first paranthesis of (66) arise from the vertical nonuniformity of the currents and are usually neglected in longshore current calculations [see, *e.g.*, Mei (1983, eq. 5.3, p. 471)]. The last term in the first paranthesis is either neglected (Mei) or absorbed in the definition of the radiation stress (Phillips 1977).

The $\int_{-h_0}^{\bar{\zeta}} UV\,dz$ term in (66) represents the cross-shore transport of longshore momentum by the cross-shore current and the $\overline{\int_{\zeta_t}^{\zeta} u_w V}$ term represents the net cross-shore transport of longshore momentum by the waves. Hence, in combination, these terms represent the total cross-shore

transport of longshore momentum by the waves and the currents. It is easily verified that in a situation with no net cross-shore mass flux these terms oppose each other and exactly cancel in the special case of depth-uniform longshore currents.

Svendsen & Putrevu showed that the paranthetic term in (66) may be written as

$$\int_{-h_0}^{\bar{\zeta}} UV dz + \overline{\int_{\zeta_t}^{\zeta} u_w V + v_w U dz} = -D_c h \frac{dV_m}{dx} + F_1 V_m + F_2 \tag{68}$$

where D_c (the dispersion coefficient) is given by

$$D_c = \frac{1}{h} \int_{-h_0}^{\bar{\zeta}} U \int_z^{\bar{\zeta}} \frac{1}{\nu_t} \int_{-h_0}^{z} U \, dz \, dz \, dz \tag{69}$$

F_1 and F_2 are similar, but less important, coefficients determined by the vertical structure of the currents. Substitution of (67) and (68) into (66) shows that the D_c term adds to the lateral mixing caused by the turbulent Reynolds stresses. It turns out that for typical surf zone conditions, $D_c \gg \nu_t$. For example, Figure 8 shows typical cross-shore variations of the dispersion and turbulent eddy viscosity coefficients. It is clear from this figure that $D_c \gg \nu_t$ which means that lateral mixing is totally dominated by the dispersion mechanism in the nearshore.

The calculations described by Svendsen & Putrevu lead to the conclusion that the lateral structure of nearshore currents is controlled by the vertical structure of those currents. While this result is somewhat surprising, analogues of this result for the lateral spreading of contaminants in shear flows are well known [see, *e.g.*, Fischer *et al.* (1979), Chapter 4].

One of the important consequences of this result is that it unifies (at least for the alongshore uniform situation) the estimates of the magnitude of the eddy viscosity in the surf zone required for predictions of different phenomena such as the crosshore distribution of longshore currents and the vertical distribution of both cross-shore circulation and the longshoe current velocities. It furthermore suggests that the major part of the lateral mixing may be due to predictable nonlinear interactions, rather than turbulence effects which in the models of today are only described empirically or semi-empirically through higher-order closure models.

A current problem in longshore current modelling

Recently, the prediction of longshore currents on barred beaches has become a topic of intense research interest. The motivation for this comes from field observations showing that the strongest longshore current on beaches with sand bars often occurs in the trough between the bar and the shoreline (Bruun, 1963; Allender & Ditmars, 1981; Greenwood & Sherman, 1986; Church & Thornton, 1993; Smith *et al.*, 1993; Kuriyama & Ozaki, 1993). Efforts to reproduce this pattern on the basis of theoretical models that assume longshore uniformity result in longshore velocity profiles with two maxima, one over or close to the crest of the bar and one very close to the shoreline (several of the above quoted references and Allender *et al.*, 1978; Ebersole & Dalrymple, 1980; Larson & Kraus, 1991). Various modifications based on increasing the mixing in the trough behind the bar or adding a turbulent transport equation have been unable to significantly change

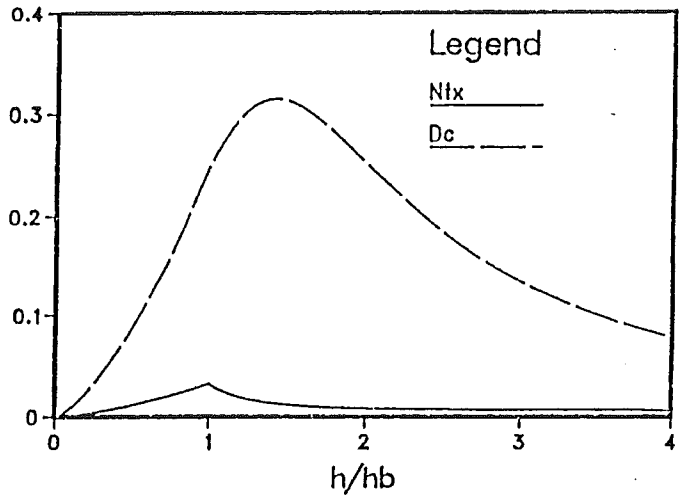

Figure 8: Cross-shore variations of the dispersion coefficient D_c and the turbulent eddy viscosity ν_t (from Putrevu & Svendsen (1992b).

this main result. [See also Church *et al.* (1994)]. It is important to emphasize, however, that the dispersive process of mixing cannot create a maximum velocity in the middle of a steady flow.

There have been a number of informal suggestions that the maximum in the trough could be attributed to longshore pressure gradients. Church & Thornton (1993) discuss this possibility. Based on the high level of correlation between the observed direction of the longshore current in the trough of the bar and the changes in the wave incidence quadrant, they argue that longshore pressure gradients are unlikely to be the cause of the observed longshore current maximum in the trough of the bar. On the other hand, recent laboratory measurements by Reniers *et al.* (1994) indicate that, under conditions of longshore uniformity, the maximum longshore current does occur over the bar crest as predicted by the models, not in the trough of the bar. This observation suggests that the longshore current maximum in the trough of the bar could be attributed to longshore variations (including longshore gradients in the mean water level) that were not adequately resolved by the instrument arrays in the field experiments. The occurrence of wave breaking also in the trough behind the bar (Lippmann & Holman 1992) and the occurence of shear waves are additional features, the effects of which yet have to be fully analyzed in this context.

Longshore Nonuniform Longshore Currents

Variations in the bottom topography will usually be associated with similar variations in the pressure (due to mean water level changes). Longshore variations of the bottom topography will therefore lead to pressure gradients in the longshore direction. The effect that longshore pressure gradients (caused either by topographic variations in the surf zone or by longshore variations in the wave height and angle at breaking) have on longshore current distributions has received very little attention even though it has been clearly demonstrated that relatively small longshore pressure gradients can drive strong longshore currents (Dalrymple 1978, Wu *et al.* 1985). For example, Wu

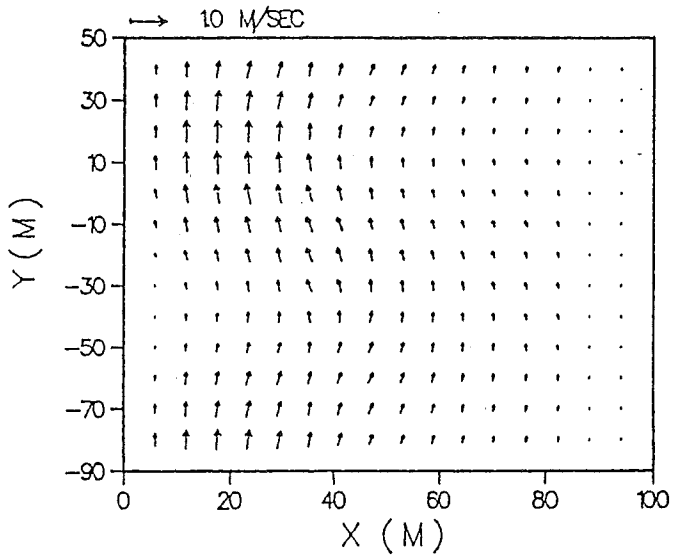

Figure 9: Calculated variations of the nearshore currents over an alongshore varying bottom topography [from Wu *et al.* (1985)].

et al. compared the predictions of a 2D surf-zone circulation model with data obtained during the NSTS experiment. Their computations showed that a topography with even a relatively small longshore variability will create substantial longshore changes in the current (Figure 9). Recently, Putrevu *et al.* (1994) extended Mei & Liu's (1977) work to study the effect of longshore topographic variability on longshore current predictions under simplified circumstances. The results confirm that longshore pressure gradients can alter the longshore currents substantially.

5.3 Depth Averaged 2D-Horizontal Models, Nearshore Circulation

Nearshore circulation is the term referring to the current patterns generated by waves, wind and tidal motion. It has long since been recognized as a major source of coastal change. The depth-averaged circulation in the horizontal plane can be described by wave-averaged models and the first of these were developed by Noda *et al.* (1974). Such models traditionally solve the wave averaged equations (7) and (14) assuming that the short-wave-averaged velocities are uniform over depth. The bottom boundary layer only influences the flow through the short-wave-averaged shear stress and is usually related to the mean velocity through a friction factor as described in Section 4. In (14) the turbulent shear stresses $\tau_{\alpha\beta}$ along the vertical sides of the water coloumn are normally modelled by means of a (lateral) eddy viscosity.

Noda *et al.* cast these equations on a special form by introducing a streamfunction ψ, but in most models the equations are solved directly for the physical variables $\bar{\zeta}$ and Q_α. The primary forcing in the equations is the variation of the radiation stresses and they are usually determined from the wave height variation using sine wave theory. As can be seen from (14), however, it is straight forward to include the effect of wind stresses as well.

Inside the surf zone, the wave height is invariably determined from (64) whereas the wave height outside the surf zone often is determined using various techniques for calculating the refraction pattern. This allows for application to arbitrary bottom topography. Examples are Noda et al (1974) who use the ray tracing method of Munk & Arthur (1952); and Ebersole & Dalrymple (1980), Wu & Liu (1985), and Watanabe (1982), who all use the fact that the wave number field is irrotational. In some cases, the models are limited to long straight beaches with longshore uniformity for which Snell's law applies which means the wave heights and directions are readily known. The model presented by Wind & Vreugdenhil (1986) is special in that it uses a two-equation turbulent closure model to determine the eddy viscosity and the dissipation of turbulent kinetic energy. The wave heights are given by (64), however, and the dissipation of wave energy is then calculated from the wave-averaged energy equation and this dissipation is used in the turbulaent closure equations to determine the eddy viscosity. The eddy viscosity is then used to determine the lateral mixing. The accuracy of this approach is unknown.

Some of the models are used for problems with a periodic bottom topography, in connection with periodicity boundary conditions at the upstream and downstream boundaries (Noda, Ebersole and Dalrymple), some analyse the circulation in a closed basin with various geometric features (Wu & Liu, Wind & Vreugdenhil, Watanabe) with similarity to the circulation patterns associated with rip currents.

In general, these models have only been used sporadically to analyze the many problems of coastal circulation which they, in spite of their simplified form, actually are capable of describing.

One of the major limitations at the moment is probably the absence of an appropriate wave driver model (see Section 8 for further discussion).

Rip Currents

Depth-averaged, 2D, horizontal models have also been used to study rip currents. These strong, seaward-oriented, jetlike flows are sometimes found emanating from the surf zone in nature [*e.g.*, Shepard *et al.* (1941), Shepard & Inman (1950), Harris *et al.* (1963), Bowen & Inman (1969), Inman *et al.* (1971), Sonu (1972), Dalrymple & Lozano (1978), to mention a few]. These seaward-oriented currents, which are often periodic in the longshore direction (*e.g.*, Figure 10), are called rip currents and are a particular source of concern to swimmers. Observations have shown that these narrow seaward oriented jets disintegrate outside the surf zone. Most of the field observations further show that the rip currents occur at locations where the wave height is the lowest. The reader is referred to Hammack *et al.* (1991) for a set of laboratory observations that provide a description of the characteristics of rip currents. For somewhat more detailed overviews of rip currents than that presented below, the reader is referred to Dalrymple (1978) and Tang & Dalrymple (1988).

A number of possible mechanisms have been proposed for the generation of rip currents. According to Tang & Dalrymple (1988), the generation models can be broadly classified into three categories:

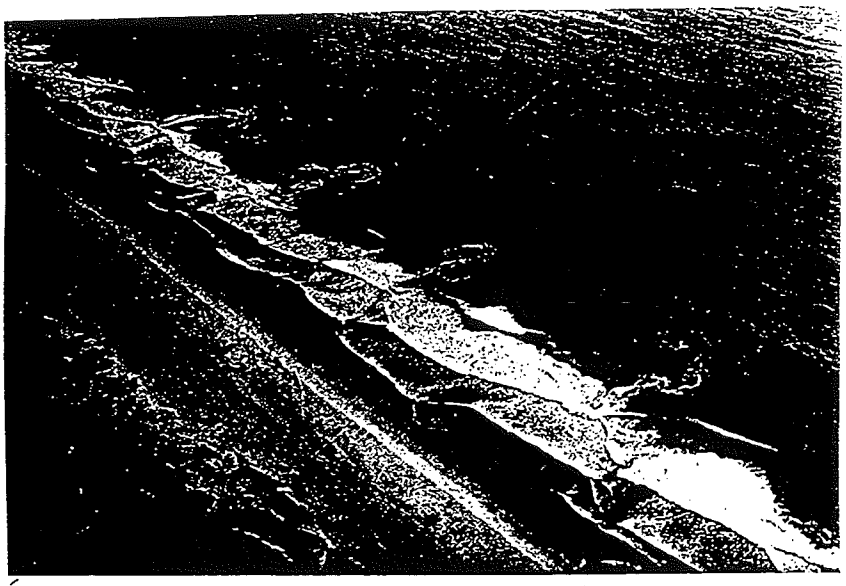

Figure 10: An example observation of rip currents (from Inman *et al.*, 1971)

1. Alongshore nonuniformities,
2. Wave-wave interactions, and
3. Instability mechanisms

In the first class of models, it is hypothesized that rip currents are generated by longshore variations of the wave height or bottom topography, which create longshore variations of the radiation stresses that in turn drive the rip currents. Bowen (1969b) showed that longshore variations of the breaker height force currents that flow seaward at locations where the wave heights are lowest. Noda (1974) used his circulation model to analyse similar situations and claimed favorable agreement with Sonu's (1972) observations. Mei & Liu (1977) developed analytical results of the circulation in the presence of a longshore perturbation of a plane beach. For simplicity, the variations were assumed to be sinusoidal. Their results showed that the direction of the circulation was contolled by the ratio of the surf zone width to the alongshore wave length of the bottom topography. Dalrymple (1978) considered the case of normally incident, non-breaking waves propagating over a longshore bar with periodic rip-channel openings. He assumed, on a heuristic basis, that the 2D horizontal flow pattern could be treated as a combination of two 1D flows: the shoreward cross-shore flow of water over the bar caused by the non-breaking waves, and the longshore flow in the trough that was fed by the cross-shore flow and hence had an increasing discharge as it approached the rip channel. His analysis indicated that gaps in alongshore bars do produce rip currents.

The presence of lateral boundaries (*e.g.*, breakwaters) introduces another type of longshore nonuniformity that can drive rip currents. Such problems have been studied theoretically by Liu & Mei (1976) and Dalrymple *et al.* (1977), and theoretically and experimentally by Wind & Vreugdenhil (1986).

The second class of models involves wave-wave interactions. Bowen (1969b) found that the

nonlinear interaction between edge waves and normally incident waves produces an alongshore variation of the wave height which, in turn, generates rip currents. This was verified in a laboratory experiment by Bowen & Inman (1969). Similarly, Dalrymple (1975) showed that two intesecting wave trains leads to a short-crested wave pattern which leads to rip currents. Experimental evidence of this driving mechanism was given by Dalrymple & Lanan (1976) and Hammack *et al.* (1991).

The third class of models hypothesizes that the state of longshore uniform wave set-up could be unstable under certain conditions and that the instability manifests itself in terms of periodic nearshore circulation cells. Early attempts at showing that steady horizontal circulation cells could be produced by perturbing the basic state of alongshore uniform set-up were made by LeBlond & Tang (1974), Hino (1974), and Iwata (1976). Miller & Barcilon (1978) and Dalrymple & Lozano (1978) questioned some the assumptions made in the earlier works and refined the models. Since these models solve eigenvalue problems, they only predict the spacing between the rips. They do not predict the strength of the rip currents. Dalrymple & Lozano included the refraction of the waves by the rip currents which provides a physical mechanism for the maintainance of the circulation cells. They also showed that their predicted rip current spacing compared favorably with field data. As pointed out by Dalrymple & Lozano, these models do not address the initiation mechanisms for the circulation patterns. They only show that circulation patterns other than that of an alongshore uniform set-up can exist on a beach.

5.4 Models with Vertical Flow Resolution

Undertow

On a long straight coast with no variation in the longshore (y-) direction, the net cross-shore mass flux $\overline{Q}_x = 0$. Nevertheless, there is a cross-shore circulation associated with the mass flux Q_{wx} near the surface. This circulation is particularly strong in the surf zone where Q_{wx} is enhanced by the breaking process. Figure 11 shows the principal flow pattern with a strong undertow (generally of the order 8-10 % of $\sqrt{gh}$) near the bottom to compensate for the shoreward mass flux of the waves.

This circulation pattern was first described quantatively by Dyhr-Nielsen & Sorensen (1970) for the special case of a barred profile and analysed theoretically for a plane beach by Svendsen (1984b). Addtional contributions to the clarification of the phenomenon have been provided by Dally & Dean (1984, 1986), Hansen & Svendsen (1984), Stive & Wind (1986), Svendsen *et al.* (1987), Okayasu *et al.* (1988), and Deigaard & Fredsoe (1989), to mention as few.

It has been found that the undertow is a balance among the forces on the fluid particle caused by a combination of the radiation stress, the pressure gradient from the sloping mean water surface, and the turbulent shear stresses. Over most of the water column, the turbulent stresses are dominated by the breaker-generated turbulence. Near the bottom, however, the turbulence intensity is small and domninated by the bottom boundary layer (Svendsen *et al.* 1987, Okayasu

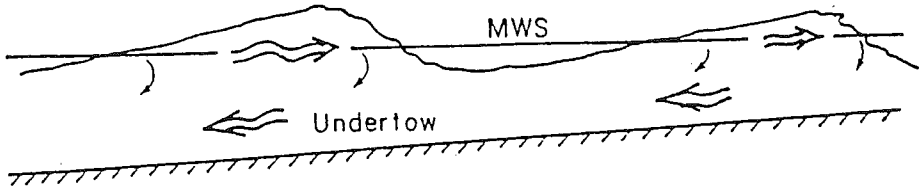

Figure 11: The circulation flow in the vertical plane including the undertow (from Svendsen, 1984b)

et al. 1988). The boundary layer also generates a steady streaming which is of no significance in the surf zone but turns out to be important outside the surf zone (Putrevu & Svendsen, 1993a). Finally, the effect of the disturbance of the wave motion due to the dacay of the wave height was addressed by Deigaard & Fredsoe (1989). In essence, they studied the modification of a sine wave motion required to transport wave energy to the region of energy dissipation, particularly the surface roller. The modification due to the variation in depth was discussed by Putrevu & Svendsen (1993a).

Basically the equation solved is obtained from (43) by assuming steady, 2D vertical flow:

$$-\frac{\partial}{\partial z}\left(\overline{w'w'}\right) = g\frac{d\bar{\zeta}}{dx} + \overline{\frac{\partial u_w^2}{\partial x}} + \overline{\frac{\partial u_w w_w}{\partial z}} \tag{70}$$

where $\overline{w'w'}$ represents the Reynolds stresses. Various approximations have been used by different authors for the terms in this equation. Generally, however, the Reynolds stresses are modeled using an eddy viscosity ν_t, which reduces (70) to

$$\frac{\partial}{\partial z}\left(\nu_t\frac{\partial U}{\partial z}\right) = g\frac{d\bar{\zeta}}{dx} + \overline{\frac{\partial u_w^2}{\partial x}} + \overline{\frac{\partial u_w w_w}{\partial z}} \tag{71}$$

In most models, the variation of ν_t is parameterized from comparison with measurement, though Deigaard *et al.* (1991) used a one equation turbulence closure to assess the variation of the eddy viscosity.

Also, the proper boundary conditions have been discussed. (71) is a second-order equation in the z-direction and hence requires two boundary conditions. The first of those is a condition for the velocity at the bottom, asssuming the bottom shear stress linked to the bottom velocity by a

friction factor f (see Section 4) which, assuming a small boundary layer thickness and sinusoidal short-wave motion, gives the condition

$$\nu_t \frac{\partial U}{\partial z}\Big)_{z=-h_0} \approx \frac{\tau_b}{\rho} = \frac{2}{\pi} f u_{wb} U_b \tag{72}$$

An alternative to (72) is to specify a variation of ν_t at the bottom that is compatible with the variation in a bottom boundary layer including $\nu_t \to 0$ at the bottom. If so, the condition $U_b = 0$ is the appropriate bottom boundary condition.

Being short-wave-averaged, the equation, only applies to the region below trough level (or mean water level – see the discussion in Section 2) The second boundary condition can either be a shear stress at the trough level (mean water level), representing the contribution of the radiation stress and pressure gradient above that level, or it can be the requirement that

$$\int_{-h_0}^{\overline{\zeta}} U dz = -Q_w \tag{73}$$

Equation (71) has the closed form solution

$$U(x,z) = \int_{-h_0}^{z} \frac{1}{\nu_{tz}} \int_{-h_0}^{z} \alpha_1 dz dz + C_1 \int_{-h_0}^{z} \frac{1}{\nu_{tz}} dz + U_b \tag{74}$$

where C_1 and U_b are integration constants, and α_1 represents the right hand side of (71). Figure 12 shows a comparison between (74) and measurements for a case where a linear variation over depth is assumed for ν_t (Okayasu *et al.*, 1988). It is important to emphasize that with such a variation of ν_t the condition $U_b = 0$ can be satisfied and (74) describes the mean flow inside the bottom boundary layer as well.

A more complete solution of (43) was given by Svendsen & Lorenz (1989) who also analysed the longshore current velocity profiles and hence established that the total current profiles essentially have a 3D structure. They also found that for the longshore currents the variation over depth is much weaker relative to the total velocity in that direction than that for the undertow. Due to the entirely different conditions (strong breaker-generated turbulence over most of the profile combined with the weak turbulence in the bottom boundary layer), the longshore current velocity profile is also distinctly different from the logarithmic velocity profile of open channel flow.

Quasi 3D models

Models for short-wave-averaged flow with resolution of the vertical current structure have been presented by DeVriend & Stive (1987), Sanchez-Arcilla *et al.* (1990), Svendsen & Putrevu (1990), Sanchez-Arcilla *et al.* (1992), Van Dongeren *et al.* (1994), among others.

Though far from equal in approach these models are all based on representing the vertical structure of the current velocities and their direction through some solution to the chosen approximation of the local wave averaged equations (43). This structure is then used in the solution

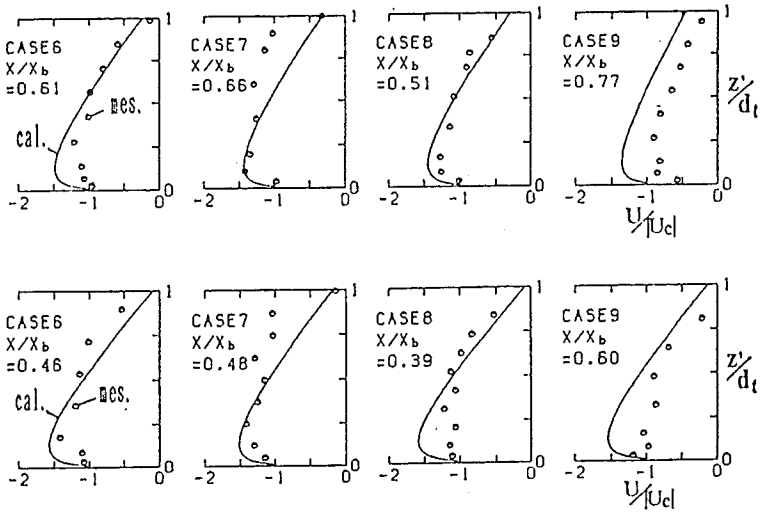

Figure 12: Comparison between measured and predicted undertow profiles on a 1/30 slope. [from Okayasu *et al.* (1988)].

for the depth-integrated, short-wave averaged equations. With the exception of Van Dongeren *et al.*, however, all the quasi 3D works assume that the interaction between currents and between currents and waves can be neglected, not only in the determination of the vertical current structure (which is probably a good approximation), but also in the integration of the 2D-horizontal equations (which is probably a less realistic assumption). Figure 13 shows as an example the variation of the 3D current velocity profiles in the time-varying flow initiated by the onset from rest of longshore currents on a long beach.

These models potentially describe so many of the nearshore circulation phenomena that substantial numerical experiments should be carried out to explore their relevance and accuracy. This would also encompass a thorough validation by comparison with laboratory and field data, which has not been carried out yet. In addition, further development of many of the model components and modification of underlying assumptions are likely to be needed. This particularly apply to addition of the dispersive mixing mechanism described in Section 5.2.

6 Infragravity Waves

6.1 Introduction

The class of gravity waves with periods ranging from about 20 to 200 seconds have come to be known as infragravity waves. The first observations of infragravity motions were reported by Munk (1949b) and Tucker (1950) who coined the term "surf beats" to denote these motions. Later field measurements (Wright *et al.* 1979, 1982; Huntley *et al.* 1981; Holman 1981; Guza & Thornton 1982, 1985; Oltman-Shay & Guza 1987; Howd *et al.* 1991 to mention a few) have

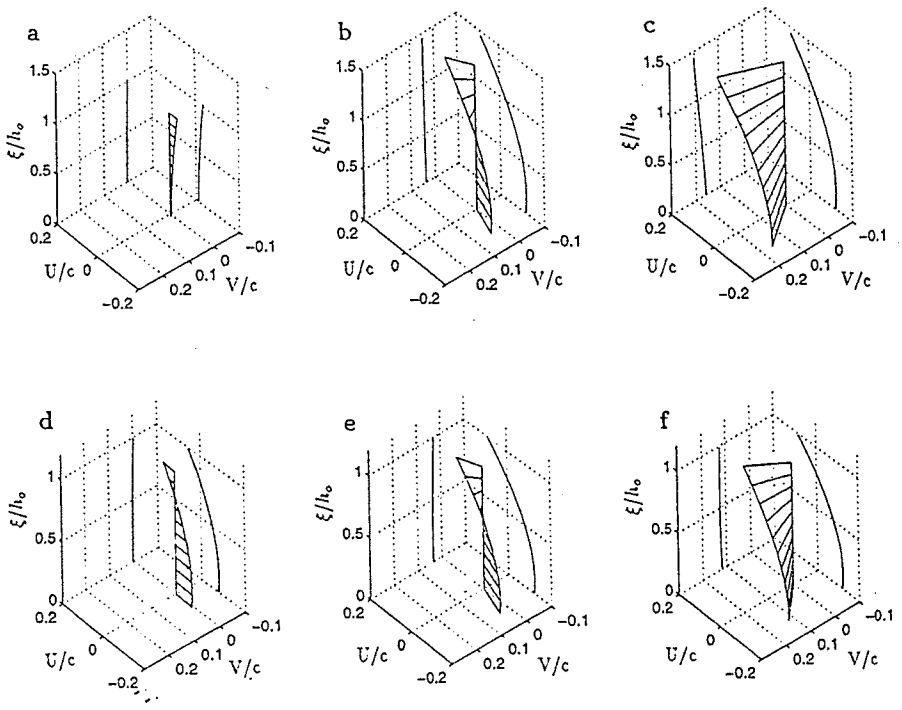

Figure 13: Three dimensional current velocity profiles at three different times during the start-up of a longshore current on a long straight beach. a) - c) at 25% of breaker depth, d) - f) near the breaker line (from Van Dongeren *et al.*, 1994).

clearly revealed that infragravity motions are ubiquitous in the nearshore. In the swash zone, the energy at infragravity frequencies often dominates, exceeding the energy at wind-wave frequencies (Wright *et al.* 1982; Guza & Thornton 1982, 1985).

Infragravity waves are solutions to the depth-integrated, short-wave-averaged equations of continuity and momentum [equations (7) and (13) of Section 2]. For the linearized versions of these equations, $\bar{Q}$ can be eliminated to yield the following equation for the infragravity surface elevation (Foda & Mei 1981, Symonds *et al.* 1982, Schäffer & Svendsen 1988)

$$\frac{\partial^2 \zeta}{\partial t^2} - \frac{\partial}{\partial x_\alpha}\left(g h_o \left(\frac{\partial \zeta}{\partial x_\alpha}\right)\right) = \frac{1}{\rho}\frac{\partial^2 S_{\alpha\beta}}{\partial x_\alpha \, \partial x_\beta} \tag{75}$$

where the radiation stress ($S_{\alpha\beta}$) could vary with time if the short-wave height varies with time (and where for convenience we have omitted the overbar on ζ).

Most of the work on infragravity motions assumes that the bathymetry does not vary in the longshore direction. Hence, the discussion below also assumes longshore uniform bottom bathymetry.

The solutions to the homogeneous version of (75) (frequently referred to as free waves) are the normal modes of oscillation on a beach. These modes are separated into two kinematically distinct classes. The first class – edge waves – have a discrete set of eigenvalues in the range $\sigma^2/g \leq k_y \leq \sigma^2/gh_x$ where σ is the frequency and k_y is the longshore wave number (Ursell 1952). The second class – leaky waves – have a continuous spectrum of eigenvalues in the range $\sigma^2 > gk_y$.

Edge waves (discussed in Section 6.2) are infragravity waves that are trapped in the nearshore region by refraction.[2] Leaky waves, on the other hand, are infragravity motions that escape back out into the deep ocean upon reflection from the shoreline.

The solutions to the inhomogeneous version of (75) represent forced infragravity motions. Offshore of the surf zone, in intermediate water depth (relative to the infragravity waves), the solution to the inhomogeneous version of (75) are referred to as bound waves. Bound infragravity waves are locally generated by the short-wave groups and propagate along with the groups (or are "bound" to the groups). The solutions for the bound waves on a horizontal bottom were given by Longuet-Higgins & Stewart (1962, 1964), Hasselmann (1962), and Gallagher (1971) [see also Bowen & Guza (1978)]. These solutions will not be discussed here. Inside the surf zone, mechanisms that cause the RHS of (75) to be non zero and hence force infragravity motions have been proposed by Symonds *et al.* (1982) and Schäffer & Svendsen (1988). These mechanisms are further discussed in Section 6.4.

[2]The reader is referred to Holman (1984) and Oltman-Shay & Hathaway (1989) for more detailed discussions than that given below of the basic solution for edge waves and to Schäffer & Jonsson (1992) for a discussion of edge wave solutions from a geometric optics standpoint.

6.2 Edge Waves

On a plane beach, the solutions for the free edge wave modes were given by Stokes (1846), Eckart (1951), and Ursell (1952). Stokes gave the solution for the so-called zero-mode edge wave [the first normal mode of oscillation of (75)]. Eckart gave the solution for all the edge wave modes assuming that the depth is shallow everywhere (relative to edge wave scales). The extension of Eckart's solution to arbitrary depth was given by Ursell who showed that edge waves follow the dispersion relationship

$$\sigma^2 = g k_y \sin[(2n+1)h_x] \tag{76}$$

where n is the mode number of the edge waves. He further showed that the wavenumbers of the edge waves are constrained to be in the range

$$\frac{\sigma^2}{g} \leq k_y \leq \frac{\sigma^2}{g h_x} \tag{77}$$

A consequence of this constraint is that no edge waves exist with wavenumbers higher than (wavelengths smaller than) those given by the mode-zero edge wave dispersion relationship.

Experimental and theoretical analysis of edge wave properties

Some of the interest in edge waves stems from the fact that they have been postulated to be responsible for many features observed on natural beaches. Examples include rip currents (Bowen & Inman 1969) and observed topographic features (Bowen & Inman 1971, Guza & Inman 1975, Bowen 1980, Guza & Bowen 1981, Holman & Bowen 1982, to mention a few).

Motivated by the possible consequences of the presence of edge waves, much effort has been spent since the 70's, trying first to prove the existence (or the lack thereof) of edge waves in a natural surf zone, later to unveil their dominant properties. Since edge waves are very difficult to generate in a controlled way in the laboratory, much of the effort has been oriented towards field data and towards theoretical modelling. While analysis of measurements from cross-shore arrays showed substantial amounts of infragravity energy in the surf zone, the presence of edge waves could not be conclusively inferred because close to the shore the cross-shore structure of the edge wave modes and leaky waves modes are very similar [see Holman (1983) for a discussion].

By analyzing the longshore structure of the infragravity motions, Huntley *et al.* (1981) provided the first compelling evidence for the presence of edge waves in a natural surf zone. They concentrated on a subset of the data collected during the NSTS experiments and demonstrated that edge waves could be detected in the measurements of the longshore currents. Based on their analysis, Huntley *et al.* concluded that "only one progressive edge wave dominates at any particular frequency." Oltman-Shay & Guza (1987) demonstrated, using synthetic data testing, that at any frequency longshore velocity variance would indeed be dominated by one edge wave mode even if all edge wave modes were present.

An extensive analysis by Oltman-Shay & Guza of the data collected during the NSTS experiments showed that edge waves were always present during these experiments. Oltman-Shay &

Guza found that the longshore current variance was dominated by low mode edge waves while the cross-shore current was dominated either by higher mode (≥ 3) edge waves or by leaky waves (because of the limitations of the data set, they were not able to distinguish between high mode edge waves and leaky waves). Their analysis suggested that all the low mode edge waves (≤ 2) had comparable amplitudes at the shoreline. Combining this with the result that the longshore velocity variance would be dominated by one edge wave mode, they showed that if all the edge wave modes have comparable shoreline amplitudes (a white spectrum), the longshore current at a particular location will be dominated by the lowest edge wave mode that is not trapped significantly shoreward of that location.

Thus, the work of Huntley *et al.* and Oltman-Shay & Guza demonstrated the presence of low mode edge waves in the surf zone. Recent work by Elgar *et al.* (1992), Herbers *et al.* (1992), and Oltman-Shay (1994) has provided evidence that high mode edge waves are also present in the surf zone.

Recent work has also clarified the effects that nonplanar bottom topography and longshore currents have on edge waves. The effect of the topography was studied by Holman & Bowen (1979), and Kirby *et al.* (1981) while Howd *et al.* (1992) and Falques & Iranzo (1992) studied the effects of the longshore current. Oltman-Shay & Howd (1993) included both these effects in a model-data comparison.

It was found that the concave beach face that often is found in nature substantially influences both the dispersion relationship and the cross-shore structure of the edge waves (Holman & Bowen 1979, Oltman-Shay & Howd 1993). In particular, Holman & Bowen showed that 1) assuming a simple beach profile could result in errors up to 100% for the wave number and 2) the relative importance of the longshore and cross-shore velocities is altered by the beach concavity. Oltman-Shay & Howd showed that the influence of concave beach faces on the cross-shore structure of the edge waves occurs even at frequencies where the wave numbers are not substantially altered by the topography. An example calculation showed that assuming a simple beach profile could overestimate the shoreline cross-shore velocity variance by a factor of four (see their Figure 5).

These results are similar to the findings of Kirby *et al.* (1981) who investigated the behavior of edge waves in the presence of longshore sand bars. Their results indicated that, for the topographies they considered, the edge wave dispersion relationship was unaltered from the plane beach case. They suggested that, on barred beaches, the edge wave dispersion relationship is controlled by the mean beach slope (as opposed to the class of beach profiles investigated by Holman & Bowen). Their calculations also demonstrated that even though the dispersion relationship is unchanged, the cross-shore structure of the edge waves is considerably altered by the presence of sand bars. They found that the edge wave surface elevation (cross-shore velocity) profile adjusts itself so that the antinodes (nodes) occur at the bar locations.

Restricting themselves to longshore currents that have $V_{max}/c < 1$, Howd *et al.* (1992) demonstrated that the cross-shore shapes of the edge waves are sensitive to the presence of a current. They found that for typical field conditions the presence of the longshore current could change the alongshore wave number of the edge waves by up to 30%. This result suggests that when

analyzing field measurements it is important to account for the presence of the longshore current. An important consequence of the presence of the longshore current is that it introduces an asymmetry: the longshore wavenumber increases for a longshore current opposing the edge wave propagation and the wavenumber decreases for a longshore current in the direction of edge wave propagation [see also Oltman-Shay & Guza (1987)]. These results were confirmed by Oltman-Shay & Howd (1993) who showed that the effect of the shear in the longshore current is particularly dramatic on the longshore velocity of edge waves. Their results also showed that for the NSTS data sets assuming a simple topography (plane beach) and neglecting longshore currents could lead to errors as high as 45% while estimating the variances at the shoreline.

Falques & Iranzo (1992) removed the restriction on the strength of the longshore current imposed by Howd *et al.* and demonstrated that, in most cases, the offshore extent of the edge waves increases (decreases) when they propagate against (with) the current. They also demonstrated analytically that in the case of edge waves propagating with a strong longshore current (strong enough so that $V = c$ at some locations), the edge wave is tightly bound to the shore – it cannot extend seaward of the location where $V = c$. Similarly, there is a region in wavenumber-Froude number space in which edge waves cannot propagate against the current.

Field observations suggest that many quantities characterizing infragravity waves in the surf zone (wave heights, velocity fluctuations, run up) are well correlated with the offshore incident wave height (Holman 1981; Guza & Thornton 1982, 1985; Holman & Sallanger 1985; Howd *et al.* 1991) which points at the short wave motion as one of the sources of the infragravity waves. Guza & Thornton (1982) showed that the infragravity swash amplitude varied linearly with the incident wave height. Holman & Sallanger analyzed data from a different beach and found that while the infragravity swash amplitude did depend on the offshore wave height the variation was more complicated than that found by Guza & Thornton. In particular, they suggested that the normalized (by the offshore significant wave height) infragravity swash amplitude depends on the "surf similarity" parameter for the short-wave motion. Similar results were obtained by Guza & Thornton (1985) and Howd *et al.* (1991)

Recent observations of infragravity energy offshore of the surf zone (Elgar *et al.* 1992, Herbers *et al.* 1992, Oltman-Shay 1994) may have interesting implications for the importance of surf zone forcing of infragravity motions. Elgar *et al.* show that offshore of the surf zone the locally forced bound waves contribute very little to the total infragravity energy except under the rare conditions of very energetic swell [see also Okihiro *et al.* (1992)]. This observation indicates that free (or nonlocally forced) infragravity motions are frequently the dominant source of infragravity energy offshore of the surf zone. Furthermore, Herbers *et al.* showed that for swell conditions the free infragravity energy at an offshore location is well correlated with and depends linearly on the incident swell energy [see also Oltman-Shay (1994)]. Present models of surf zone generation of infragravity motions (discussed below) suggest that the infragravity energy generated in the surf zone will exhibit a linear dependence on the incident wave energy. Thus, at present there are strong indications that a substantial amount of infragravity wave generation may be taking place in the surf zone.

6.3 Generation of Infragravity Waves in the Surf Zone

Offshore of the surf zone, Longuet-Higgins & Stewart (1962, 1964), Hasselmann (1962), Gallagher (1971) and Bowen & Guza (1978) showed that the group structure of the incident wave field could generate infragravity motions. Surf zone generation of one-dimensional infragravity motions (leaky waves) was considered by Symonds *et al.* (1982) and Schäffer & Svendsen (1988). The first of these works considered the generation of infragravity motions due to temporal variations of the break point on a plane beach due to the variations of the short-wave height. Briefly, Symonds *et al.* argued that since individual waves in a group have different heights, they are likely to begin breaking at different locations and have different heights at the initial location of breaking. Hence, the position of the break point is a function of time. Symonds *et al.* assumed that the group structure of the incident waves is destroyed by the breaking process. Thus, the long-wave generation only takes place in a narrow region which is termed as the "zone of initial breaking."

The time variation of the break point generates long waves at the group period (and its higher harmonics) which are radiated both shorewards and seawards. The shoreward radiated waves are reflected at the shoreline and radiate back out seaward. The model of Symonds *et al.* predicts that the amplitude of this outgoing free wave is a strong function of the frequency of the long wave. On the other hand, the shoreline amplitude of the infragravity motion was found not to exhibit frequency dependence. They attribute this lack of resonant behavior to the radiation of energy seaward. Symonds & Bowen (1984) extended the model to include the presence of an alongshore bar.

The following heuristic argument is often used to explain the mechanism proposed by Symonds *et al.* (1982). As discussed previously, the loss of the cross-shore-directed momentum flux due to the breaking process is balanced by changes in the mean water level (set-up). Bowen *et al.* (1968) showed that, under simplified circumstances, this set-up is proportional to the breaking wave height. Thus, temporal variations of the breaker height lead to corresponding temporal variations of the set-up. This time-varying set-up is equivalent to the infragravity wave surface elevation.

Looking at the other extreme situation relative to Symonds *et al.*, Schäffer & Svendsen (1988) assumed that all the waves in a group begin to break at the same fixed location. This implies that all the groupiness of the incident wave field is transmitted into the surf zone. Hence they could study the generation of infragravity waves due to wave height variation throughout the surf zone, and in parallel with Symonds *et al.* they found that the groupiness of the broken-wave field generates of long waves at the group period. This generation can be very strong, and they quantified the strength of the generation in terms of a "reflection coefficient" defined as the ratio between the outgoing free long wave and the incoming bound long wave.

In Schäffer & Svendsen's model, a bound long wave generated by the Longuet-Higgins & Stewart mechanism is assumed incident at the seaward boundary of the model domain. Further generation of the long waves takes place as the incident short waves shoal over the sloping bottom and after they break. Thus, the "reflection coefficient" could more descriptively be termed as the

"amplification factor" for the nearshore region because it measures how much the incident (set-down) waves are amplified by the nearshore processes of shoaling and breaking. They find that the "reflection coefficient" can attain values as high as 25-30 suggesting very strong generation of infragravity wave energy in the nearshore region. Though some of this amplification is due to the long-wave generation on the slope, Schäffer & Svendsen found that a large fraction of the outgoing free long wave is indeed generated in the surf zone.

Schäffer (1993) combined the models of Symonds *et al.* (1982) and Schäffer & Svendsen to allow for both a time variation of the break point as well as a partial transmission of the groupiness into the surf zone. He compared the predictions of this model with laboratory measurements of Kostense (1984) and found qualitative agreement. He also found that his model consistently overpredicts the long wave generation. Schäffer attributes this overprediction to his neglect of bottom friction and the feedback between the long waves and the short waves.

An extension of this model to two horizontal dimensions (Schäffer 1994) shows that for small angles of incidence leaky waves are generated whereas for larger angles of incidence edge waves are generated by the same mechanisms. Schäffer (1994) compared his predictions of the amplitude of the forced edge wave with the laboratory measurements of the same quantity by Bowen & Guza (1978). Schäffer's solution assumes a beach of infinite alongshore extent so that the edge waves generated are steady state, whereas the experiments conducted by Bowen & Guza had limited longshore extent which prevented the development of steady edge waves. This is probably the reason why Schäffer predicts much higher edge wave amplitudes than the laboratory measurements of Bowen & Guza.

Definitive field evidence for the importance (or the lack thereof) of the generating mechanisms discussed above has not yet been presented. On the one hand, List (1992) solved (7) and (14) numerically assuming that the groupiness of the short-wave field is destroyed by the breaking process (thus his calculations do not include the Schäffer & Svendsen mechanism). He compared his numerical solutions with field data and found that for the particular data set he was working with the long wave generated by the Symonds *et al.* mechanism is secondary to the bound long waves. This contradicts the results discussed in Section 6.2 of Herbers *et al.* (1992) and Oltman-Shay (1994), who suggested that the linear correlation between the variances of the infragravity and swell waves indicates that the free infragravity wave variance is predominantly generated in the nearshore. As List pointed out, however, his conclusions are only valid for the conditions of the data set that he analyzed. For example, his numerical experiments show that the importance of the long-wave forced by the break point variations increases with increasing beach slope.

It is also pointed out here that the theories of Symonds *et al.* and Schäffer & Svendsen assume that the forcing wave groups are steady. This will usually not be true in practice. Thus, these theories have to be extended to unsteady wave groups before their importance in the field can be determined.

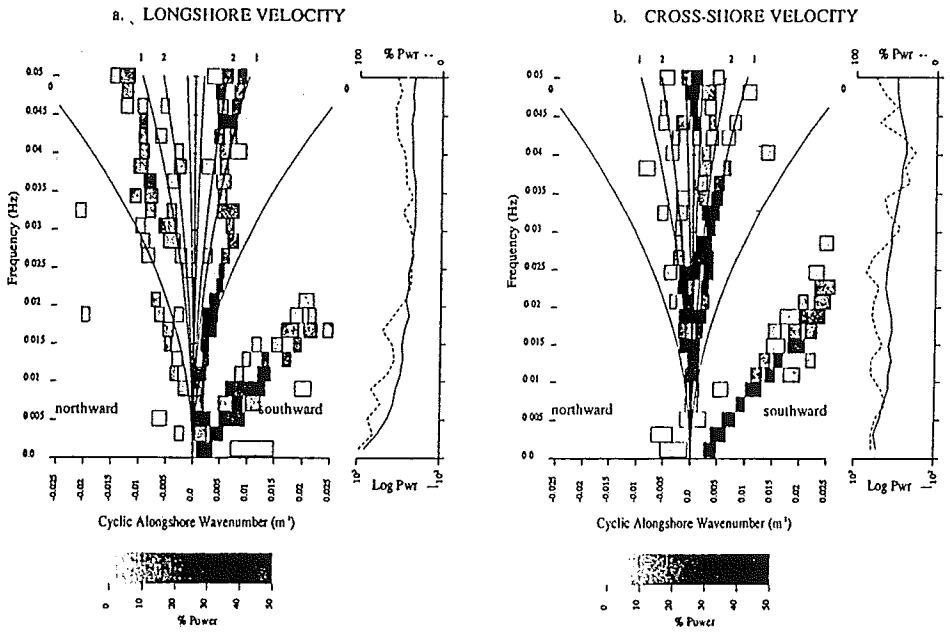

Figure 14: An estimated frequency-alongshore wavenumber spectrum for low frequency motions in the surf zone [from Oltman-Shay *et al.* (1989)].

6.4 Velocity Profiles in Infragravity Waves

Putrevu & Svendsen (1993b) and Svendsen & Putrevu (1994b) presented a local solution for the vertical structure of the velocity profiles in infragravity waves. Their solution predicts that if there is no local forcing of infragravity waves, then the infragravity velocity profiles will not exhibit vertical structure. On the other hand, the solution predicts that the infragravity waves will exhibit vertical structure if there is local forcing of infragravity waves by short-wave variations. Thus the Putrevu & Svendsen solution predicts vertical structure in the infragravity velocity field in the zone of initial breaking as well as throughout the surf zone if the groupiness of the incident short-wave field is not completely destroyed by the breaking process.

7 Shear Waves

Analysis of data collected during the SUPERDUCK field experiment (Crowson *et al.* 1988) by Oltman-Shay *et al.* (1989) demonstrated the presence of low frequency wave like oscillations of the longshore currents. These oscillations were found to be progressive longshore with longshore wave lengths and periods of order 100 m and 100 s, respectively. For example, Figure 14 shows a typical longshore wavenumber-frequency spectrum of the longshore velocity (see Oltman-Shay *et al.* for details). The solid lines in this figure represent the dispersion relationships of the various edge wave modes and the rectangular boxes show the locations and half power bandwidth of the estimated variance peaks. [3]

[3]Though shear waves were first detected in the data collected during the SUPEDUCK field experiment, there is evidence that these motions were also present during the NSTS experiments (Dodd *et al.* 1992).

As discussed under "Edge Waves," no surface gravity motions exist for wavenumbers higher than (wavelengths lower than) those given by the mode-0 edge wave relationship. The field data in Figure 14 clearly shows the presence of motions with wavenumbers too short to be surface gravity motions (the linear dispersion line to the right of the mode-0 edge wave curve in Figure 14). Thus, Oltman-Shay *et al.* concluded that the observed concentration of variance located outside the mode-0 edge wave curve is derived from a source other than surface gravity motions. The motions represented by these dispersion lines have come to be known as shear waves. Observations have shown that shear waves can be quite energetic with velocity amplitudes greater than $30cm/s$ (Oltman-Shay *et al.*) and can contribute up to 33 % of the longshore current variance (Howd *et al.* 1991).

Oltman-Shay *et al.* demonstrated that shear waves have the following characteristics:

1. They are almost non dispersive and propagate in the direction of the longshore current;
2. Their kinematics are closely linked to the strength of the mean longshore current;
3. The speed of propagation is in the range $0.5V_p$ - V_p where V_p is the peak longshore current magnitude;
4. Longshore and cross-shore velocity components are in quadrature phase; and
5. The magnitude of the longshore current does not affect the range of observed wavenumbers.

Bowen & Holman (1989) suggested that shear waves may be generated by a shear instability of the mean longshore current profile. Using very simple variations of the longshore current and bottom topography, Bowen & Holman showed that longshore currents could be potentially unstable over a range of wave numbers. They further demonstrated that the predicted scales compared favorably with those observed in the field. Bowen & Holman also found that the critical parameter in the stability problem is the shear on the seaward face of the longshore current. Subsequent work by Dodd & Thornton (1990), Dodd *et al.* (1992), Putrevu & Svendsen (1992a), and Falques & Iranzo (1994) have confirmed these results.

Dodd *et al.* solved the stability equation using measured longshore current and depth profiles and compared the predictions of the instability theory (frequencies and wavenumbers) to measurements made during NSTS and SUPERDUCK experiments. They found that the predictions of the instability theory compared well with the observations at SUPERDUCK. With the NSTS data set, however, Dodd *et al.* found that the instability theory predicted no shear wave generation whereas field data clearly showed the presence of shear waves.

Putrevu & Svendsen (1992a) studied the effect of bottom topography on the stability characteristics of longshore currents. Their results demonstrated that the bottom topography has a considerable influence on the stability characteristics. For example, their results showed that the presence of a bar significantly destabilizes the longshore current. This, in turn, suggests that shear

waves are more likely to be observed on barred beaches rather than on plane slopes (a conjecture already made by Bowen & Holman).

Falques & Iranzo (1994) presented an efficient numerical solution to the stability problem which relaxes the rigid lid assumption made in the theoretical works mentioned above. They also included the effects of a horizontal eddy viscosity (neglected in all previous works) and bottom friction (also included by Dodd *et al.*) using very simple formulations. Their results confirm the strong influence the bottom topography has on the stability characteristics. They also demonstrate that the rigid lid assumption is reasonable as long as the maximum local Froude number (the maximum value of $V/\sqrt{gh}$) is much smaller than unity. (This requirement is met in most cases.) They also found that both the bottom friction and horizontal eddy viscosity can substantially influence the stability characteristics of longshore currents.

Recently, Reniers *et al.* (1994) presented laboratory experiments on the generation of shear waves. They generated longshore uniform longshore currents using a technique of recirculation similar to that used by Visser (1984). Preliminary results indicate the presence of shear waves on barred beaches. Whereas on a plane slope, they find that shear waves do not develop. Given the close connection between this finding and the theoretical predictions, it seems likely that the generating mechanism of shear waves may indeed be the instability mechanism proposed by Bowen & Holman.

The theoretical studies described above consider the linear stability problem only. Because of the exponential growth predicted by the linear theory, all of the above-mentioned analyses will only be applicable at the initial stage when the assumption of linearity is applicable. While it may be reasonable to expect that the scales predicted by the linear theory are applicable also later in the development process, a nonlinear analysis is required to predict the amplitude and the spatial structure. Preliminary reports of such nonlinear analyses are just now appearing in the literature (Allen *et al.* 1994, Ozkan & Kirby 1994).

Finally it should also be mentioned that alternative mechanisms for the generation of very low frequency motions have been proposed by Fowler & Dalrymple (1990) and Shemer *et al.* (1991). The mechanism of Fowler & Dalrymple essentially consists of the interaction of two wave trains of slightly different frequencies. They show that such an interaction produces a migrating rip current which has a low frequency signature in the wavenumber-frequency space that is similar to that of the shear waves. Similarly, Shemer *et al.* show that a side band instability of the incident gravity waves could lead to a modulation of the longshore component of the radiation stress which, in turn, causes a modulation of the longshore current that resembles the observed motions.

8 Comprehensive Quasi-3D Models

Comprehensive quasi-3D nearshore models can be developed on the basis of the equations presentented above though this has not yet been fully accomplished. The basis for such models is the following:

A model that solves the depth-integrated, short-wave-averaged equations would represent a nearshore circulation model that would be capable of predicting wave-generated current motions under general topographical and wave conditions. If such a model is combined with a state-of-the-art model that predicts short-wave transformations over abritrary bottom bathymetry, the resulting model system would represent a comprehensive nearshore model that will be capable of predicting waves and wave-averaged motions in the nearshore. Though significant strides are being made these years such general model systems still remain to be developed [see Van Dongeren *et al.* (1994) for a preliminary report on a comprehensive circulation model]. Such models will be extensions of the models discussed under "Quasi 3D models" in Section 5, and they would consist of the following elements:

1. A component that solves the depth-integrated, short-wave-averaged equations of horizontal momentum giving the 2D horizontal variation of the current/infragravity-wave pattern. Early versions of such model components were developed by Noda (1974), Noda *et al.* (1974), Ebersole and Dalrymple (1980), Kirby & Dalrymple (1982), Wu & Liu (1985), and Winer (1988).

2. A component that evaluates the analytical solutions to the vertical distribution of horizontal velocities of the time varying currents – which are equivalent to the particle velocities of the infragravity waves – and calculates the quantities required for the 2D-horizontal equations under 1) (for example, the lateral dispersive mixing coefficient).

3. A short-wave transformation model ("wave driver") that describes the propagation of the short-waves in the computational region with particular emphasis on predicting the radiation stresses, mass fluxes, etc. of the short period wave motion. This element essentially determines the short-wave forcing for the equations in 1) and 2).

There are several important features of the 2D-horizontal equations which are worth mentioning.

First of all, virtually no approximations have been made in the derivation of these equations other than the approximations already embedded in the fundamental Reynolds equations for turbulent fluid motion. Thus they automatically satisfy the (exact) nonlinear boundary conditions at the bottom and the free surface, which means that the effects of bottom friction, wind stresses on the surface, etc. can be incorporated exactly to the extent we need for the sediment processes. This means that we can expect the solutions to these equations to include the actual processes that occur on a real beach even if we do not presently have simple representations (or even knowledge) of these processes.

Secondly, today it is possible to solve these equations using state of the art numerical techniques, which are both highly efficient and accurate, without omitting any of the terms in the equations. This means that we can expect such solutions to include the actual processes that occur on a real beach even if we do not presently have simple representations or even knowledge about these processes. An example of this is the discovery of the importance that the nonlinear current-current and wave-current interactions have for the lateral mixing (Putrevu & Svendsen, 1992b, Svendsen & Putrevu, 1994a) described in Section 5.3, and actually the original discovery of the radiation stress as a term in the equations is another example.

The opportunities this accuracy provides have not been fully explored yet in the literature.

The second, integral part of such a model system is the solution for the vertical structure of the currents and infragravity wave particle velocities. As described elsewhere in this paper it has been found that in the nearshore region currents not only vary in strength over the depth (as one would expect) but often also have widely different directions at the bottom and at the surface. This variation also changes quite dramatically over time. An example was shown in Fig 13, Section 5.3.

The lateral dispersive mixing mechanism crucially depends on this vertical variation. However, in addition to influencing the horizontal distribution of the currents (as the mixing does), the vertical variation clearly will also have a strong effect on how currents and long waves move sediments. This is because the major part of the sediment transport occurs close to the bottom, whereas the water transport involved in the large scale current and infragravity-wave patterns is determined by the flow over the entire depth. Hence the sediment motion generated by the currents and infragravity-waves will in general be in a different direction than what is perceived as the current direction if only the depth averaged motion is considered. Therefore the resolution of the vertical current structure is crucial not only for the correct modelling of the hydrodynamics but also to the sediment transport processes. Hence if a sediment-transport component is added to such a quasi-3D model we can expect that the model will include these mechanisms.

The third component of the model system is the socalled wave driver. The wave driver can in principle be any short-wave transformation model. Though there are exceptions (see, e.g., Watanabe 1982, Winer 1988), most nearshore models published so far have assumed a long straight coast. The wave driver is then replaced simply by Snell's law, which provides the wave pattern, plus the wave-averaged energy equation, which provides the wave height variation. This approach is not possible on a general bathymetry and for general wave input. A bonafide wave propagation model is needed as a driver for such cases.

Since the short-wave time scale is much smaller than the time scale of the nearshore circulation, the short-wave models suitable as drivers must be reasonably crude in order to be computationally economical, and they are not accurate enough to actually predict the nearshore circulation. They must, however, include a reasonably accurate description of wave-height decay in the surf-zone. Their primary function here is to provide the driving forces for the circulation in the form of radiation stress, mass flux etc. With this as forcing, the nearshore circulation can then be determined by solution of the equations described under 1) and 2). However, if a sediment-transport

component is added to the quasi-3D model the wave driver would have the additional function of providing sufficient information about the local wave particle velocity near the bottom to make it possible to determine the net effect of the oscillatory part of the sediment motion.

9 Concluding Remarks

In this review, we have attempted to discuss the present state of understanding of surf zone hydrodynamics. As has hopefully become clear from this review, considerable progress has been made in the last thirty years even though there are still many areas where our understanding is far from satisfactory.

Wave breaking provides the forcing for larger scale motions in the surf zone. It is therefore probably both somewhat ironic as well as unfortunate that at the present time there exists no satisfactory theory to describe breaking and broken waves in the surf zone. This is currently a topic of intense research interest and we are confident that substantial progress will be made in the near future.

While our overall understanding of wave-induced nearshore circulations seems to be fairly sound, there are a number of phenomena that clearly require further study. These include, but are not limited to, quantitatively accurate predictions of rip currents; the predictions of longshore currents on barred beaches; and the importance of alongshore inhomogenieties on nearshore circulations. Once again, these topics are currently being pursued by a number of investigators, and we expect considerable progress in the near future.

Recent work has demonstrated that the surf zone is an important region for the generation of infragravity motions. While the present indications are that a substantial fraction of the infragravity energy seems to be generated in and near the surf zone, the existing models of surf zone generation of infragravity motions have not been verified.

Shear waves seem to be amenable to an interpretation as a manifestation of an instability of the longshore current. Ongoing work on the nonlinear development of the instability and the importance of wave group forcing on these motions promises to yield interesting results.

In conclusion, the subject of surf zone hydrodynamics is at an exciting stage of development right now and we expect that many of the issues will be clarified in the near future. We may also expect that the ongoing and future work will discover phenomena which we are currently unaware of.

Acknowledgements

We wish to thank N. Kobayashi, J. Oltman-Shay and D. H. Peregrine for useful and interesting discussions. We also thank K. Verna for editing this manuscript. This effort was supported by the Army Research Office under contract number DAAL03-92-G-0016 (IAS), and the Office of Naval Research, Coastal Sciences under contract number N00014-94-C-0004 (UP). The U.S. government is authorized to produce and distribute reprints for government purposes notwithstanding any copyright notation that may appear herein.

10 References

Allen, J. S., P. A. Newberger, and R. A. Holman (1994). Nonlinear shear waves in the surf zone over plane beaches. Abstract # O12F-7, EOS Transactions, 75, p. 322.

Allender, J. H., J. D. Ditmars, W. Harrison, and R. A. Paddock (1978). Comparison of model and observed nearshore circulation. *16th Intl. Conf. Coastal Engrg.*, ASCE, 810-827.

Allender, J. H., and J. D. Ditmars (1981). Field measurements of longshore currents on a barred beach. *Coastal Engrg.*, 5, 295-309.

Banner, M. L. (1987). Surging characteristics of spilling zones of quasi-steady breaking water waves. In *IUTAM Symosium Nonlinear Water Waves*, Tokyo.

Barnes, T. C. D., D. H. Peregrine, and G. Watson (1994). Low frequency wave generation by a single wave group. *Proceedings of the international symposium: Waves - Physical and Numerical Modeling*, Vancouver, pp. 280-286.

Basco, D. R., and T. Yamashita (1986). Towards a simple model of the wave breaking transition region in surf zones. *Proceedings of the 20th International Conference on Coastal Engineering*, 955.

Battjes, J. A. (1974). Surf similarity. *Proceedings of the 14th Coastal Engineering Conference*, pp. 466-480.

Battjes, J. A. (1975). Modelling of turbulence in the surf-zone. *Proceedings of a Symposium on Modelling Techniques*, ASCE, San Francisco, pp. 1050-61.

Battjes, J. A. (1988). Surf-zone dynamics. *Annual Review of Fluid Mechanics, 20, pp. 257-293.*

Battjes, J. A., and J. P. F. M. Janssen (1978). Energy loss and set-up due to breaking of random waves. *Proc. 16th ICCE*, Hamburg, p. 569–587.

Battjes, J. A., and T. Sakai (1981). Velocity field in a steady breaker. *J. Fluid Mech.111*, 121-137.

Battjes, J. A., R. J Sobey, and M. J. F. Stive (1990). Nearshoe circulation. (in *The Sea: Ocean Engineering Science, 9*, John Wiley and Sons, 468-493.

Battjes, J. A., and M. J. F. Stive (1985). Calibration and verification of a dissipation model for random breaking waves. *Journal of Geophysical Research*, 90, pp. 9159-9167.

Bowen, A. J. (1969a). The generation of longshore currents on a plane beach. *Journal of Marine Research, 27*, pp. 206-215.

Bowen, A. J. (1969b). Rip currents, Part 1: Theoretical investigations. *Journal of Geophysical Research, 74*, pp. 5467-78.

Bowen, A. J. (1980). Simple models of nearshore sedimentation; Beach profiles and longshore bars. In *The Coastline of Canada*, Pub. 80-10, McCann, S. B. ed., Geological Survey of Canada, Ottawa.

Bowen, A. J., and R.T. Guza (1978). Edge waves and surf beat. *Journal of Geophysical Research,83*, pp. 1913-1920.

Bowen, A. J., and R. A. Holman (1989). Shear instabilities in the mean longshore current 1: Theory. *Journal of Geophysical Research,94*, pp. 18,023-18,030.

Bowen, A. J., and D.L. Inman (1969). Rip currents. Part 2, Laboratory and field experiments. *Journal Geophys. Res.*, **74**, 5479–5490.

Bowen, A. J., and D.L. Inman (1971). Edge waves and crescentic bars. *Journal Geophys. Res.*, 76, 8662.

Bowen, A.J., and D.L. Inman (1974). Nearshore mixing due to waves and wave induced currents. *Rapp. P.-v. Reun. Cons. Int.*, 167, pp. 6-12.

Bowen, A. J., D. L. Inman and V.P. Simmons (1968). Wave 'set-down' and set-up. *Journal of Geophysical Research, 73*, pp. 2569-2577.

Brocchini, M., M. Drago, and L. Ivoenitti (1992). The modeling of short waves in shallow waters. Comparison of numerical models based on Boussinesq and Serre equations. *Proceedings of 23rd International Conference on Coastal Engineering,*

Bruun, P. (1963). Longshore currents and longshore troughs. *J. Geophys. Res.*, 68, 4, 1065-1078.

Cox, D. T., N. Kobayashi, and D. L. Kriebel (1994). Numerical model verification using SUPERTANK data in surf and swash zones. *Proc. Coastal Dynamics '94.* Barcelona, Spain. (ASCE)

Cox, D. T., N. Kobayashi, and A. Wurjanto (1992). Irregular wave transformation processes in surf and swash zones. *Proc 23rd International Conference on Coastal Engineering,* Venice, Italy, ch 10, 156-169

Christoffersen, J. B., and I. G. Jonsson (1985). Bed friction and dissipation in a combined current and wave motion.*Ocean Engrg., 12*, 5, 387-423.

Church, J. C., and E. B. Thornton (1993). Effects of breaking wave induced turbulence within a longshore current model, *Coastal Engrg.*, 1-28.

Church, J. C., E. B. Thornton, and J. Oltman-Shay (1994). Mixing by shear instabilities of the longshore current. Submitted to *J. Geophys. Res.*

Crowson, R. A., W. A. Birkemeier, H. M. Klein, Harriet, and H. C. Miller (1988). SUPERDUCK Nearshore Processes Experiment: Summary of Studies CERC Field Research Facility. Technical Report CERC-88-12, US Army Engineer Waterways Experiment Station, Coastal Engineering Research Center, Vicksburg, MS.

Dally, W. R. (1990). Random breaking waves: a closed form solution for planar beaches. *Coastal Engineering, 14.* 233-263

Dally, W. R. (1992). Random breaking waves: field verification of a wave by wave algorithm for engineering application. *Coastal Engineering, 16*, 369-397.

Dally, W. R., and R. G. Dean (1984). Suspended sediment transport and beach profile evaluation. Journal of Waterway, Port, Coastal and Ocean Engineering, ASCE, 110, pp. 15-33.

Dally, W. R., and R. G. Dean (1986). Discussion of Mass flux and undertow in a surf zone" by I. A. Svendsen, *Coastal Engineering*, 10, pp. 289-299.

Dally, W. R., R. G. Dean, and R. A. Dalrymple (1985). Wave height variation across beaches of arbitrary profile. *Journal of Geophysical Research, 90*, pp. 11,917-11,927.

Dalrymple, R. A. (1975). A mechanism for rip current generation on an open coast. *Journal Geophys. Res.*, **80**, 24, 3485–3487.

Dalrymple, R. A. (1978). Rip currents and their causes. *16th Int'l. Conf. Coastal Engineering*, Hamburg, 1414–1427.

Dalrymple, R. A., R. A. Eubanks, and W. A. Birkemeier (1977). Wave-induced circulation in shallow basins. *J. Waterway, Port, Coastal, and Ocean Engineering*, **103**, 117–135.

Dalrymple, R. A., and G. A. Lanan (1976). Beach cusps formed by intersecting waves, *Bull. Geol. Soc. Amer.*, 87, pp. 57-60.

Dalrymple, R. A. and C. J. Lozano (1978). Wave current interaction models for rip currents. *Journal Geophys. Res.*, **83**, C12, 6063.

Davis, A. G., R. L. Soulsby, and H. L. King (1988). A numerical model of the combined wave current bottom boundary layer. *Journal of Geophys. Res.*, 93, 491–508.

deVriend, H. J., and M. J. F. Stive (1987). Quasi-3D modelling of nearshore currents. *Coastal Engineering, 11*, pp. 565-601.

Deigaard, R., and J. Fredsoe (1989). Shear stress distribution in dissipative water waves. *Coastal Engineering*, 13, 357-378.

Deigaard, R., P. Justesen, and J. Fredsoe (1991). Modelling undertow by a one equation turbulence model. *Coastal Engineering, 15*, 431-458.

Dodd, N., J. Oltman-Shay, and E. B. Thornton (1992). Shear instabilities in the longshore current: A comparison of observation and theory. *Journal of Physical Oceanography.*

Dodd, N., and E.,B. Thornton (1990). Growth and energetics of shear waves in the nearshore. *Journal of Geophysical Research, 95*, pp. 16,075-083.

Duncan, J. H. (1981). An experimental investigation of wave breaking produced by a towed hydrofoil. *Proceedings of the Royal Society of London, Series A, 377*, pp. 331-348.

Dyhr-Nielsen, M., and T. Sorensen (1970). Some sand transport phenomena on coasts with bars. Proceedings of the 12th Coastal Engineering Conference, pp. 855-66.

Ebersole, B. A., and R.A. Dalrymple (1980). Numerical modeling of nearshore circulation. *Proc. 17^{th} Intl. Conf. Coastal Eng.*, ASCE, 2710-2725.

Eckart, C. (1951). Surface waves on water of variable depth. Wave Report # 100, Scripps Institution of Oceanography,.

Elder, J. W. (1959). The dispersion of marked fluid in turbulent shear flow. Journal of Fluid Mechanics, 5, pp. 544-560.

Elgar, S., T.H.C. Herbers, M. Okihiro, J. Oltman-Shay, and R. T. Guza (1992). Observations of infragravity waves. *Journal of Geophysical Research, 97*, pp. 15,573-15,577.

Falques, A., and V. Iranzo (1992). Edge waves on a longshore shear flow. *Physics of Fluids*, A4, pp. 2169-2190.

Falques, A., and V. Iranzo (1994). Numerical simulation of vorticity waves in the nearshore. *Journal of Geophysical Research, 94*, pp. 825-841.

Fischer, H. B. (1978). On the tensor form of the bulk dispersion coefficient in a bounded skewed shear flow. *Journal of Geophysical Research, 83*, pp. 2373-2375.

Fischer, H.B., E. J. List, R. C. Y. Koh, J. Imberger, and N. H. Brooks (1979). *Mixing in Inland and Coastal Waters.* Academic Press Inc., Orlando. 483 pp.

Foda, M. A., and C. C. Mei (1981). Nonlinear excitation of long trapped waves by a group of short swells. *J. Fluid Mechanics*, 111, pp. 319-345.

Fowler, R. E., and R.A. Dalrymple (1990). Wave group forced nearshore circulation. *Proceedings of the 22nd Coastal Engineering Conference*, pp. 729-742.

Fredsoe, J. (1983). The turbulent boundary layer in combined wave-current motion, *Journal of Hydraulic Engineering*, 110, 8, pp. 1103-1120.

Fredsoe, J., and R. Deigaard (1993). Mechanisms of coastal sediment transport. World Scientific, Singapore. 369 pp.

Gallagher, B. (1971). Generation of surf beat by nonlinear wave interactions. Journal of Fluid Mechanics, 49, pp. 1-20.

Galvin, C. J. (1968). Breaker type classification on three laboratory beaches. *J. Geophys. Res.*, **73** , 12.

Galvin, C. J. (1972). Wave brewaking in shallow water. In *Waves on beaches and resulting sediment transport*, ed. R.E. Meyer, 413-456.

George, R., R. E. Flick, and R. T. Guza (1994). Observations of turbulence in the surf-zone. *Journal of Geophysical Research*, 99, C1, pp. 801-810.

Grant, W. D., and O. S. Madsen (1979). Combined wave and current interaction with a rough bottom. *J. Geophysical Research, 84* , 1797-1808.

Greenwood, B., and D.J. Sherman (1986). Longshore current profiles and lateral mixing across the surf zone of a barred nearshore. *Coastal Engrg.*, 10, 149-168.

Grilli S. T., I. A.Svendsen, and R. Subramanya (1994). Breaking criterion and characteristics for solitary waves on plane beaches. (Submitted for publicationn)

Guza, R. T., and A. J. Bowen (1981). On the amplitude of beach cusps. *J. Geophysical Research*, 86, 4125.

Guza, R. T., and D. L. Inman (1975). Edge waves and beach cusps. *J. Geophysical Research*, 80, 2997.

Guza, R. T., and E. B. Thornton (1982). Swash oscillations on a natural beach. *Journal of Geophysical Research*, 87, pp. 483-491.

Guza, R.T., and E.B. Thornton (1985). Observations of surf beat. *Journal of Geophysical Research, 90, C2*, pp. 3161-3171.

Hammack, J., N. Scheffner, and H. Segur (1991). A note on the generation and narrowness of periodic rip currents. *Journal of Geophysical Research*, 96, C3, pp. 4909-4914.

Hansen, J. B. (1990). Periodic waves in the surf-zone: Analysis of experimental data. *Coastal Engineering, 14*, pp. 19-41.

Hansen, J. B., and I. A. Svendsen (1984). A theoretical and experimental study of the undertow. *Proceedings of the 19th Coastal Engineering Conference*, Houston, pp. 2246-2262.

Harris, T.F. W., J.M. Jordan, W.R. McMurray, C.J. Verwey and F.P. Anderson (1963). Mixing in the surf zone. *International Journal of Air and Water Pollution,7*, pp. 649-667.

Hasselman, K. (1962). On the non-linear energy transfer in gravity wave spectrum, Part 1, General theory. *Journal of Fluid Mechanics*, 12, 481-500.

Hattori, M., and T. Aono (1985). Experimental study on turbulence structures under spilling breakers. In *The Ocean Surface*, Toba and Mitsuyasu, eds. Reidel Publ. Comp., Dordrecht, pp. 419-424.

Herbers, T.H.C., S. Elgar, R.T. Guza, and W.C. O'Riley (1992). Infragravity frequency motions on the shelf. *Proceedings of the 23rd Coastal Engineering Conference*, pp. 846-859.

Hibberd, S., and D.H. Peregrine (1979). Surf and runup on a beach: a uniform bore. *J.FLuid Mech. 95*,323-345.

Hino, M. (1974). Theory on the formation of rip currents and cuspidal coast. *Proceedings of the 14th International Conference on Coastal Engineerng*, pp. 901-919.

Holman, R. A. (1981). Infragravity energy in the surf zone. Journal of Geophysical Research, 86, pp. 6442-6450.

Holman, R. A. (1983). Edge waves and the configuration of the shoreline. *The CRC Handbook of Coastal Processes and Erostion*, CRC Press, Boca Raton, pp. 21-33.

Holman, R. A., and A. J. Bowen (1979). Edge waves over complex beach profiles. *Journal of Geophysical Research*, 84, pp. 6330-6346.

Holman, R. A., and A. J. Bowen (1982). Bars, bumps and holes: models for generation of complex beach topography. *J. Geophysical Research*, 87, 457.

Holman, R. A., and A. H. Sallenger (1985). Set-up and swash on a natural beach, *J. Geophysical Research*, 90, pp. 945-953.

Horikawa, K., and C. T. Kuo (1966). A study of wave transformation inside the surf-zone. *Proceedings of the 10th Coastal Engineering Conference*, pp. 217-233.

Howd, P. A., A. J. Bowen, and R. A. Holman (1992). Edge waves in the presence of strong longshore currents. *Journal of Geophysical Research*, 97, pp. 11,357-11,371.

Howd, P. A., J. Oltman-Shay, and R. A. Holman (1991). Wave variance partitioning in the trough of a barred beach. Journal of Geophysical Research, 96, pp. 12781-12795.

Huntley, D. A., R. T. Guza, and E. B. Thornton (1981). Field observations of surf beat, Part I: Progressive edge waves. *Journal of Geophysical Research, 86*, pp. 6451-6466.

Hwang,L.-S., and D. Divoky (1970). Breaking wave setup and decay on gentle slopes. *Proceedings 12th Int. Conf. coastal Engineering*, chap 23, 377-389.

Inman, D. L., R. J. Tait, and C. E. Nordstrom (1971). Mixing in the surf zone. *Journal of Geophysical Research, 76*, pp. 3493-3514.

Irribarren, C. R., and C. Nogales (1949). Protection des Ports II, *Comm. 4, 17th Int. Navig. Congr., Lisbon*, pp. 31-80.

Iwata, N. (1976). Rip current spacing. *Journal of the Oceanographical Society of Japan*, 32, pp. 1-10.

Janssen, P. C. M. (1986). Laboratory observations of the kinematics in the aerated region of breaking waves. *Coastal Engineering*, 9, 5, pp. 453-477.

Jonsson, I. G. (1966). Wave boundary layers and friction factors. *Proceedings of the 10th Coastal Engineering Conference*, pp. 127-148.

Jonsson, I. G., and N. A. Carlsen (1976). Experimental and theoretical investigations in an oscillatory turbulent boundary layer. *Journal of Hydraulic Research, 14 1)*, pp. 45-60.

Karambas, Th., Y. Krestenitis, and C. Koutitas (1990). A numerical solution of the Boussinesq equations in the inshore zone. *Hydrosoft 3*, 1, 34-37.

Karambas, Th., and C. Koutitas (1992). A breaking wave propagation model based on the Boussinesq equations. *Coastal Engineering 18*, 1-19.

Kirby, J.T., and R. A. Dalrymple (1982). Numerical modelling of the nearshore region.*Research Report # CE-82-24*, Ocean Engineering Program, Department of Civil Engineering, University of Delaware.

Kirby, J.T., R. A. Dalrymple, and P. L.-F. Liu (1981). Modification of edge waves by barred beach topography. *Coastal Engineering 5*, pp 35-49.

Kobayashi, N., G. S. DeSilva, and K. D. Watson (1989). Wave transformation and swash oscillation on gentle and steep slopes. *J. Geophys. Res.*, C1, 951 - 966.

Kobayashi, N., and A. Wurjanto (1992). Irregular wave setup and runup on beaches. *Journal of Waterway, Port, Coastal, and Ocean Engineering 118*, 368-386.

Kostense, J. K. (1984). Measurements of surf beat and set-down beneath wave groups. *Proceedings of the 19th Coastal Engineering Conference*, pp. 724-740.

Kuriyama, Y., and Y. Ozaki (1993). Longshore current distribution on a bar-trough beach – Field measurements at HORF and numerical model", *Report of Port and Harbour Research Institute Vol 32, No 3.*

Larson, M., and N.C. Kraus (1991). Numerical model of longshore current for bar and trough beaches. *J. Waterway, Port, Coastal, and Ocean Eng.* 117, 4, ASCE, 326-347.

LeBlond, P. H., and G. L. Tang (1974). On energy coupling between waves and rip currents. *Journal of Geophysical Research*, 79, pp. 811-816.

LeMehaute, B. (1962). On non-saturated breakers and wave run-up. Proceedings of the 8th Coastal Engineering Conference, pp. 77-92.

Lippmann, T.C., and R.A. Holman (1992). Wave breaking in the trough of a natural sand bar. *Trans. Amer. Geophys. Union*, 73, p. 256.

Lin, J.-C., and D. Rockwell (1994). Instantaneous structure of a breaking wave. *Phys. Fluids*, 6(9), 2877–2879.

List, J. H. (1992). A model for the generation of two dimensional surf beat.*Journal of Geophysical Research, 97, C4*, pp. 5623-5635.

Liu, P.L.-F., and R. A. Dalrymple (1978). Bottom frictional stresses and longshore currents due to waves with large angles of incidence. *Journal of Marine Research, 36*, pp. 357-375.

Liu, P. L.-F., and C. C. Mei (1976). Water motions on a beach in the presence of a breakwater. Parts 1 and 2. *Journal of Geophysical Research*, 81, pp. 3079-3094.

Longuet-Higgins, M. S. (1970). Longshore currents generated by obliquely incident sea waves. Parts 1 and 2. *Journal of Geophysical Research, 75*, pp. 6778-6789 and pp. 6790-6801.

Longuet-Higgins, M. S. (1973). A model of flow separation at a free surface. *Journal of Fluid Mechanics*, 57, pp. 129-148.

Longuet-Higgins, M. S., and R. W. Stewart (1962). Radiation stress and mass transport in gravity waves with application to 'surf-beats'. *Journal of Fluid Mechanics, 8*, pp. 565-583.

Longuet-Higgins, M.S., and R.W. Stewart (1964). Radiation stress in water waves, a physical discussion with application. *Deep Sea Research, 11*, pp. 529-563.

Longuet-Higgins, M. S., and J. S. Turner (1974). An entraining plume model of a spilling breaker. *Journal of Fluid Mechanics*, 63, pp. 1-20.

Mei, C. C. (1983). The applied dynamics of ocean surface waves. John Wiley and Sons, New York, 740 pp.

Mei, C.C., and P.L.-F. Liu (1977). Effects of topography on the circulation in and near the surf-zone – linear theory. *Estuarine and Coastal Marine Science*, 5, pp. 25-37.

Miller, C., and A. Barcilon (1978). Hydrodynamic instability in the surf zone as a mechanism for the formation of horizontal gyres. *Journal of Geophysical Research*, 83, C8, 4107-4116.

Munk, W. H. (1949a). The solitary wave theory and its application to surf problems. Annals of the New York Academy of Sciences, 51, pp. 376-424.

Munk, W. H. (1949b). Surf beats. *Transactions of the American Geophysical Union, 30*, pp. 849-854.

Munk, W. H., and R. S. Arthur (1952). Wave intensity along a refracted ray in gravity waves. *Nat. Bur. Sand Circ 521*, Washington, D.C.

Nadaoka, K. (1986). A fundamental study on shoaling and velocity field structure of water waves in the nearshore zone. Doctoral dissertation, Department of Civil Engineering, Tokyo Institute of Technology, Tokyo.

Nadaoka, K., M. Hino, and Y. Koyano (1989). Structure of the turbulent flow field under breaking waves in the surf zone. Journal of Fluid Mechanics, 204, pp. 359-387

Nadaoka, K., and T. Kondoh (1982). Laboratory measurements of velocity field structure in the surf zone by LDV. Coastal Engineering in Japan, 25, pp. 125-145

Nielsen, P. (1992). Coastal bottom boundary layers and sediment transport. *World Scientific, Singapore.*

Noda, E. K. (1974). Wave induced nearshore circulation. *Journal Geophys. Res.*, **79**, 4097–4106.

Noda, E. K., C. J. Sonu, V. C. Rupert, J. I. Collins (1974). Nearshore circulations under sea breeze conditions and wave-current interactions in the surf-zone. *Tetra Tech Rep. TC-149-4.*

Okayasu, A. (1989). Characteristics of turbulence structure and undertow in the surf-zone. Doctoral dissertation, Department of Civil Engineering, University of Tokyo, 119 pp.

Okayasu, A., T. Shibayama, and K. Horikawa (1988). Vertical variation of undertow in the surf-zone. *Proceedings of the 21st Coastal Engineering Conference*, pp. 478-491.

Okihiro, M., R. T. Guza, and R. J. Seymour (1992). Bound infragravity waves. *Journal of Geophysical Research*, 97, pp. 11453-11469.

Oltman-Shay, J. (1994). Evidence of high mode edge waves. Submitted to *J. Geophys. Res.*

Oltman-Shay, J., and R. T. Guza (1987). Infragravity edge wave observations on two California beaches. *Journal of Physical Oceanography, 17*, pp. 644-663.

Oltman-Shay, J., and K. Hathaway (1989). Infragravity energy and its implications in nearshore sediment transport dynamics. Report # CERC-89-6, Waterways Experiment Station, Vicksburg, MS.

Oltman-Shay, J., and P. A. Howd (1993). Edge waves on nonplanar bathymetry and alongshore currents: A model and data comparison. *Journal of Geophysical Research, 98*, pp. 2495-2507.

Oltman-Shay, J., P. A. Howd, and W. A. Berkemeier (1989). Shear instabilities of the mean longshore current 2: Field observations. *Journal of Geophysical Research, 94*, pp. 18,031-042.

Ozkan, H. T., and J. T. Kirby (1994). Numerical Study of finite amplitude shear wave instabilities. Abstract # O12F-6, EOS Transactions, 75, p. 322.

Packwood, A., and D. H. Peregrine (1980). The propagation of solitary waves and bores over a porous bed. *Coastal Engineering3*, 221-242.

Packwood, A. (1983). The influence of beacgh porosity on wave uprush ands backwash. *Coastal Engineering7*, 29-40.

Peregrine, D. H. (1983). Breaking waves on beaches. *Annual Review of Fluid Mechanics*, 15, pp. 149-178.

Peregrine, D. H., and I. A. Svendsen (1978). Spilling breakers, bores and hydraulic jumps. *Proceedings of the 16th International Conference on Coastal Engineering*, pp. 540-550.

Phillips, O. M. (1977). The dynamics of the upper ocean. Cambridge University Press, 336 pp.

Putrevu, U., J. Oltman-Shay, and I. A. Svendsen (1994). Effect of alongshore nonuniformities on longshore current predictions. Submitted to the *J. Geophys. Res.*

Putrevu, U., and I. A. Svendsen (1992a). Shear instability of longshore currents: A numerical study. *Journal of Geophysical Research, 97*, pp. 7283-7303.

Putrevu, U., and I. A. Svendsen (1992b). A Mixing Mechanism in the Nearshore Region. *Proc. of the 23rd International Conference on Coastal Engineering*, pp. 2758-2771.

Putrevu, U., and I. A. Svendsen (1993a). Vertical Structure of the Undertow Outside the Surf-Zone. *J. Geophys. Res.* 98, C12, 22707 - 22716.

Putrevu, U., and I. A. Svendsen (1993b). Infragravity velocity profiles in the surf-zone. *Journal of Geophysical Research*, under review.

Reniers, A. J. H. M., J. A. Battjes, A. Falques and D. A. Huntley (1994). Shear wave laboratory experiment. Proceedings of the international symposium: Waves – Physical and Numerical Modelling, Vancouver, pp. 356-365.

Sanchez-Arcilla, A., F. Collado, M. Lemos, and F. Rivero (1990). Another quasi-3D model for surf zone flows. *Proc. of the 22nd Coastal Engineering Conference* Chap 24. 316-329.

Sanchez-Arcilla, A., F. Collado,, and A. Rodrigues (1992). Vertically varying velocity field in Q-3D nearshore circulation. *Proc. of the 23nd Coastal Engineering Conference.* Chap215, 2811-2824.

Schäffer, H. A. (1993). Infragravity waves induced by short-wave groups. *Journal of Fluid Mechanics, 247*, pp. 551-588.

Schäffer, H. A. (1994). Edge waves forced by short-wave groups. Journal of Fluid Mechanics, 259, pp. 125-148.

Schäffer, H. A., and I.G. Jonsson (1992). Edge waves revisited. *Coastal Engineering*, 16, pp. 349-368.

Schäffer, H. A., and I. A. Svendsen (1986). Boundary layer flow under skew waves. Progress Report # 64, Institute of Hydrodynamics and Hydraulic Engineering, Technical University of Denmark, pp. 13-23.

Schäffer, H. A., and I. A. Svendsen (1988). Surf beat generation on a mild slope beach. *Proc. of the 21st International Conference on Coastal Engineering*, pp. 1058-1072.

Schäffer, H. A.,R. Deigaard, P. A. Madsen (1992). A two-dimwnsional surf zone model based on the Boussinesq equations. *Proc. of the 23st International Conference on Coastal Engineering*

Schäffer, H. A., P. A. Madsen, and R. Deigaard (1993). A Boussinesq model for waves breaking in shellow water. *Coastal Engineering, 20*, 185-202.

Shemer, L., N. Dodd and E. B. Thornton (1991). Slow-time modulation of finite depth nonlinear water waves: Relation to longshore current oscillations. *Journal of Geophysical Research*, 96, pp. 7105-7113.

Shepard, F. P., K. O. Emery, and E. C. LaFond (1941). Rip currents: A process of geological importance, *J. Geology*, 49, pp. 337-369.

Shepard, F. P., and D. L. Inman (1950). Nearshore circulation. *Proceedings of the 1st International Conference on Coastal Engineerng*, pp. 50-59.

Sleath, J. F. A. (1984). Sea bed mechanics. *John Wiley and Sons*, 335pp.

Smith, J. M., M. Larson, and N. C. Kraus (1993). Longshore current on a barred beach: Field measurements and calculation. *J. Geophys. Res.*, 98, C12, pp. 22,717-22,731.

Sonu, C. J. (1972). Field observations of nearshore circulation and meandering currents. *Journal of Geophysical Research*, 77, pp. 3232-3247.

Stive, M. J. F. (1980). Velocity and pressure field of spilling breakers. *Proceedings of the 17th International Conference on Coastal Engineerng*, pp. 547-566.

Stive, M. J. F. (1984). Energy dissipation in waves breaking on gentle slopes. *Coastal Engineering, 8*, pp. 99-127.

Stive, M. J. F., and H.G. Wind (1982). A study of radiation stress and set-up in the nearshore region. *Coastal Engineering,6*, pp. 1-26.

Stive, M. J. F., and H.G. Wind (1986). Cross-shore mean flow in the surf-zone. *Coastal Engineering, 10*, pp. 325-340.

Stokes, G. G. (1846). Report on recent researches in hydrodynamics. Report of the British Asscociation. Also in *Mathematical and Physical Papers (Collected)*, 1880, pp. 157-187.

Svendsen, I. A. (1984a). Wave heights and set-up in a surf-zone. *Coastal Engineering, 8*, pp. 303-329.

Svendsen, I. A. (1984b). Mass flux and undertow in a surf-zone. *Coastal Engineering, 8*, pp. 347-365.

Svendsen, I. A. (1987). Analysis of surf zone turbulence. *Journal of Geophysical Research, 92*, pp. 5115-24.

Svendsen, I. A., and R.S. Lorenz (1989). Velocities in combined undertow and longshore currents. *Coastal Engineering,13*, pp. 55-79.

Svendsen, I. A., and P. A. Madsen (1984). A turbulent bore on a beach. *Journal of Fluid Mechanics*, 148, pp. 73-96.

Svendsen, I. A., P. A. Madsen, and J. B. Hansen (1978). Wave characteristics in the surf-zone. *Proceedings of the 16th Coastal Engineering Conference*, pp. 520-539.

Svendsen, I. A., and U. Putrevu (1990). Nearshore circulation with 3-D profiles. *Proc. of the 22nd Coastal Engineering Conference* , pp. 241-254.

Svendsen, I. A., and U. Putrevu (1993). Surf-zone wave parameters from experimental data. *Coastal Engineering, 19*, pp. 283-310.

Svendsen, I. A., and U. Putrevu (1994a). Nearshore mixing and dispersion. *Proc. Roy. Soc. Lond. A., 445*, pp. 1-16.

Svendsen, I. A., and U. Putrevu (1994b). Velocity structure in IG-waves. *Proc Int. Symp. Waves - Physical and Num,erical Modelling* Vancouver, Aug 21-24, 346-355.

Svendsen, I. A., H. A. Schäffer and J. B. Hansen (1987). The interaction between the undertow and boundary layer flow on a beach. *Journal of Geophysical Research, 92*, pp. 11,845-11,856.

Symonds, G., and A. J. Bowen (1984). Interaction of nearshore bars with incoming wave groups. *Journal of Geophysical Research*, 89, C2, pp. 1953-1959.

Symonds, G., D. A. Huntley, and A. J. Bowen (1982). Two dimensional surf-beat: Long wave generation by a time-varying break point.*Journal of Geophysical Research, 87, C1*, pp. 492-498.

Synolakis, C. E., and J. E. Skjelbreia (1993). Evolution of the maximum amplitude of solitary waves on plane beaches. *J. Waterway,Port,Coastal, and Ocean Engineering 119*, (3), 323-342.

Synolakis, C. E. (1987). The runup of solitary waves. *J. Fluid Mechanics 185*, 523-545.

Tallent, J. R., T. Yamashita, and Y. Tsuchiya (1989). Field and laboratory measurements of large scale eddy formation by breaking waves. In *Water Wave Kinematics*, Torum, A., and O. T. Gudmestad eds. NATO ASI Series E: Applied Sciences, 178, pp. 509-523.

Tang, E., and R. A. Dalrymple (1988). Rip currents and wave groups. Nearshore Sediment Transport, R. J. Seymour, ed., Plenum Publishing Corporation, pp. 205-230.

Taylor, G. I. (1954). The dispersion of matter in a turbulent flow through a pipe. *Proceedings of the Royal Society of London. Series A*, 219, pp. 446-468.

Thornton, E. B. (1970). Variation of longshore current across the surf zone. *Proceedings of the 12th Coastal Engineering Conference*, pp. 291-308.

Thornton, E. B. (1979). Energetics of breaking waves within the surfe zone. *Journal of Geophysical Research*, 84, C8, pp. 4931-4938.

Thornton, E. B., and R. T. Guza (1982). Energy saturation and phase speeds measured on a natural beach. *Journal of Geophysical Research*, 87, C12, pp. 9499-9508.

Thornton, E. B., and R. T. Guza (1983). Transformation of wave height distribution. *Journal of Geophysical Research*, 88, C10, pp. 5925-5938.

Thornton, E. B., and R. T. Guza (1986). Surf-zone longshore currents and random waves: Field data and models. *Journal of Physical Oceanography, 16*, pp. 1165-1178.

Ting, F. C. K., and J. T. Kirby (1994). Observation of undertow and turbulence in a laboratory surf zone. *Coastal Engineering*, 24, pp. 51-80.

Trowbridge, J. H., and O. S. Madsen (1984). Turbulent wave boundary layers, parts 1 and 2. *Journal of Geophysical Research, 89*, pp. 7989-8007.

Tucker, M. J. (1950). Surf beats: sea waves of 1 to 5 minute period. *Proceedings of the Royal Society of London, A, 202*, pp. 565-573.

Ursell, F. (1952). Edge waves on a sloping beach. *Proceedings of the Royal Society of London, A, 214*, pp. 79-97.

van Dongeren, A. R., F. E. Sancho, I. A. Svendsen, and U. Putrevu (1994). Quasi 3D modeling of infragravity waves. *Proc 24th Intl. Conf. Coastal Engrg.*, in press.

van Dorn, W. G. (1976). Set-up and run-up in shoaling breakers. *Proceedings of the 15th International Conference on Coastal Engineering*, pp. 738-751.

Visser, P. J. (1982). The proper longshore current in a wave basin. Report no. 82-1, Communications on Hydraulics, Department of Civil Engineering, Delft University of Technology, 86 pp.

Visser, P. J. (1984). A mathematical model of uniform longshore currents and comparison with laboratory data. Communications on Hydraulics. Report 84-2, Department of Civil Engineering, Delft University of Technology, 151 pp.

Watanabe, A. (1982). Numerical models of nearshore currents and beach deformation. *Coastal Engrg. Jpn.*, 25, pp. 147-161.

Watson, G., and D. H. Peregrine (1992). Low frequency waves in the surf zone. *Proceedings of the 23rd International Conference on Coastal Engineering,* pp. 818-831.

Watson, G., D. H. Peregrine, and E. F. Toro (1992). Numerical solution of the shallow water equations on a beach using the weighted average flux method. *Compuational Fluid Dynamics*, 1, pp. 495-502.

Whitford, D. J. (1988). Wind and wave forcing of longshore currents across a barred beach. Doctoral dissertation. Naval Postgraduate School. 205 pp.

Wind, H. G., and C. B. Vreugdenhil (1986). Rip current generation near structures. *Journal of Fluid Mechanics*, 171, pp. 459-476.

Winer. H. S. (1988). Numerical modeling of wave-induced currents using a parabolic wave equation. UFL/COEL-TR/080, Department of Coastal and Oceanographic Engineering, University of Florida.

Wright, L. D., J. Chappell, B. G. Thom, M. P. Bradshaw, and P. Cowell (1979). Morphodynamics of reflective abd dissipative beach and inshore systems: southeastern Australia, *Marine Geology*, 32, 105.

Wright, L. D., R. T. Guza, and A. D. Short (1982). Dynamics of a high energy dissipative surf-zone. Marine Geology, 45, pp. 41-62.

Wu, C.-S., and P. L-F. Liu (1985). Finite element modeling of nonlinear coastal currents. *J. Waterway, Port, Coastal, and Ocean Eng.* 111, 2, ASCE, pp. 417-432.

Wu, C.-S., E. B. Thornton, and R. T. Guza (1985). Waves and longshore currents: Comparison of a numerical model with field data. *J. Geophys. Res.*, 90, pp. 4951-4958.

Zelt, J. A. (1991). The run-up of non breaking and breaking solitary waves. *Coastal Engineering*, 15, pp. 205-246.